

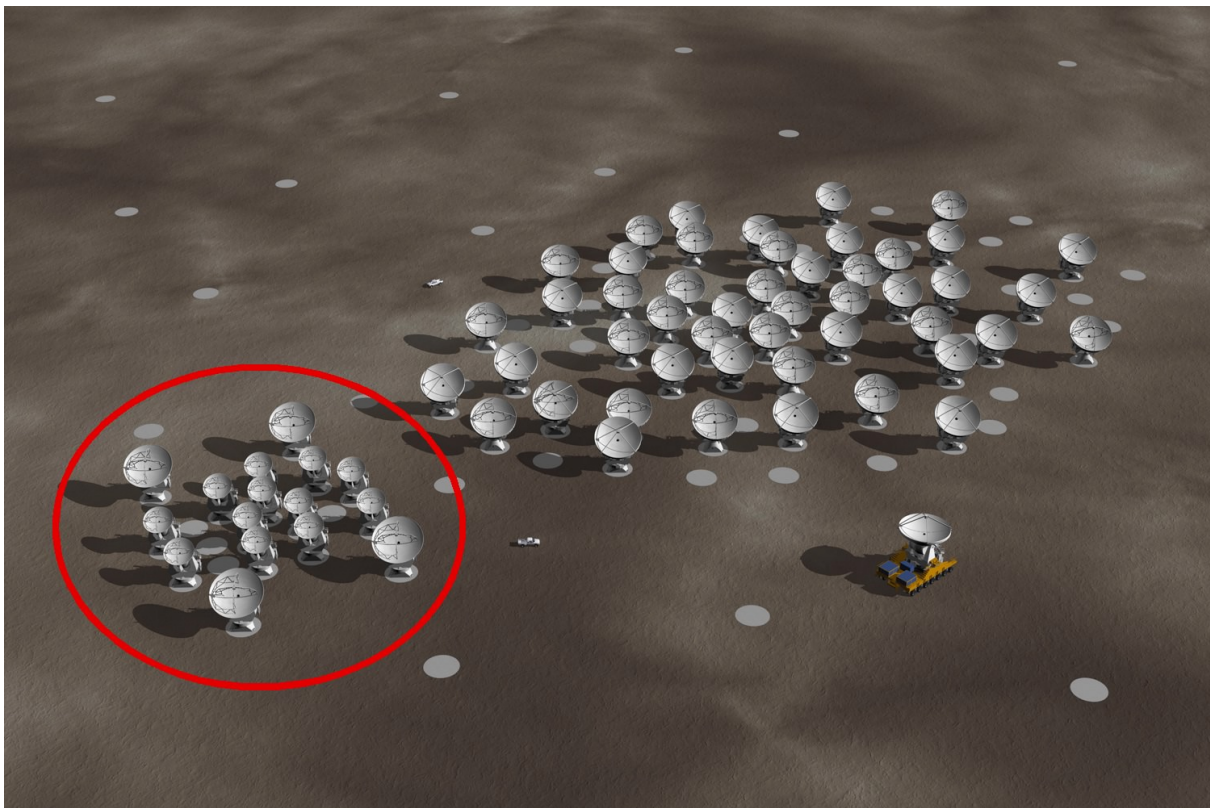
The ALMA simulator in GILDAS

Jérôme PETY

IRAM & Obs. de Paris



Identity card



Type An ALMA/ACA/SD imaging simulator.

Original goal Imaging study of the impact of ACA on the wide-field capabilities of ALMA.

Today goal Scientific preparation of ALMA.

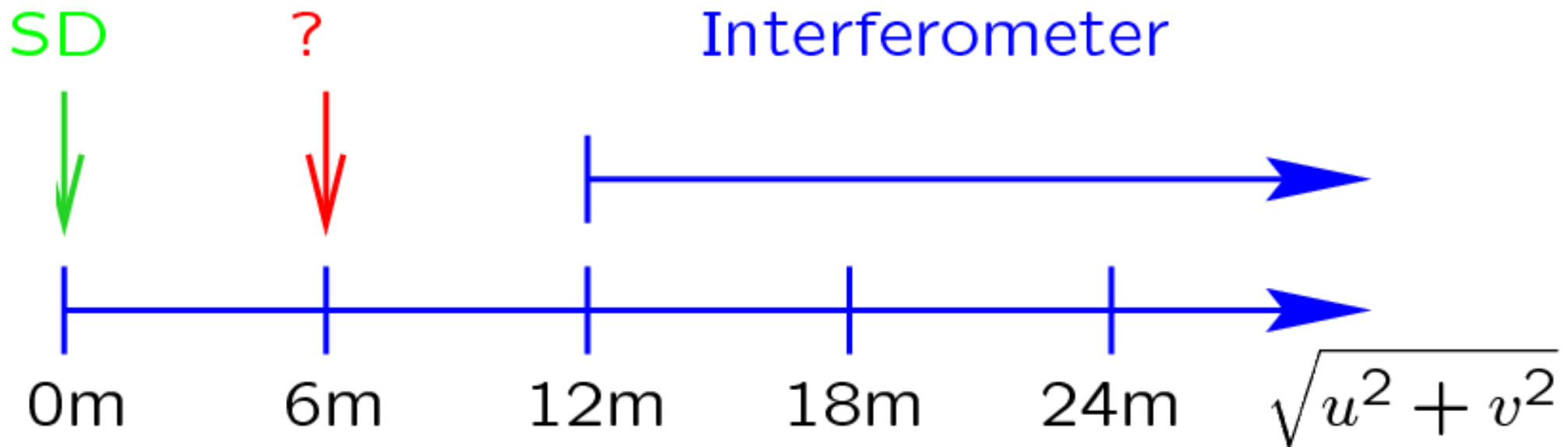
Creation date 2000-2001.

Detailed description ALMA memo #398.

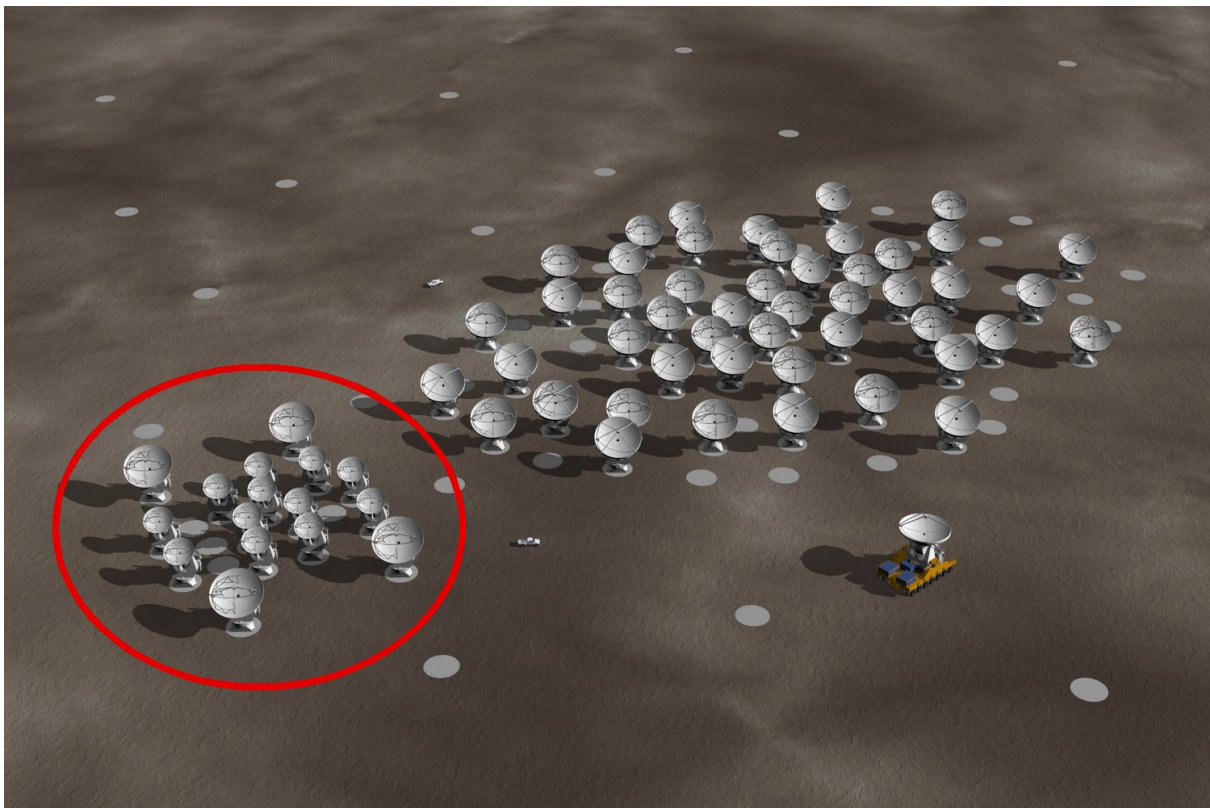
Authors Pety, Gueth & Guilloteau.

Why the Atacama Compact Array?

- ALMA field of view: 9" at 690 GHz and 27" at 230 GHz;
- ~ 25% of observations will require:
 - Bigger field of view;
 - Large dynamic of scale;
 - ⇒ Mosaicking;
- Interferometer = bandpass instrument;
⇒ Low spatial frequencies are filtered;
- ALMA antennas can be used in total power mode ⇒ zero spacing;
- Highest influence of pointing errors at 6 m.



Identity card



Type An ALMA/ACA/SD imaging simulator.

Original goal Imaging study of the impact of ACA on the wide-field capabilities of ALMA.

Today goal Scientific preparation of ALMA.

Creation date 2000-2001.

Detailed description ALMA memo #398.

Authors Pety, Gueth & Guilloteau.

Identity card (cont'ed)

Distribution

- With the GILDAS softwares
<http://www.iram.fr/IRAMFR/GILDAS>
- Inside the MAPPING program
`shell-prompt> mapping @ alma`

Implementation

1. Engines in FORTRAN95.
2. Glued together by SIC scripts.
3. Widget interface.

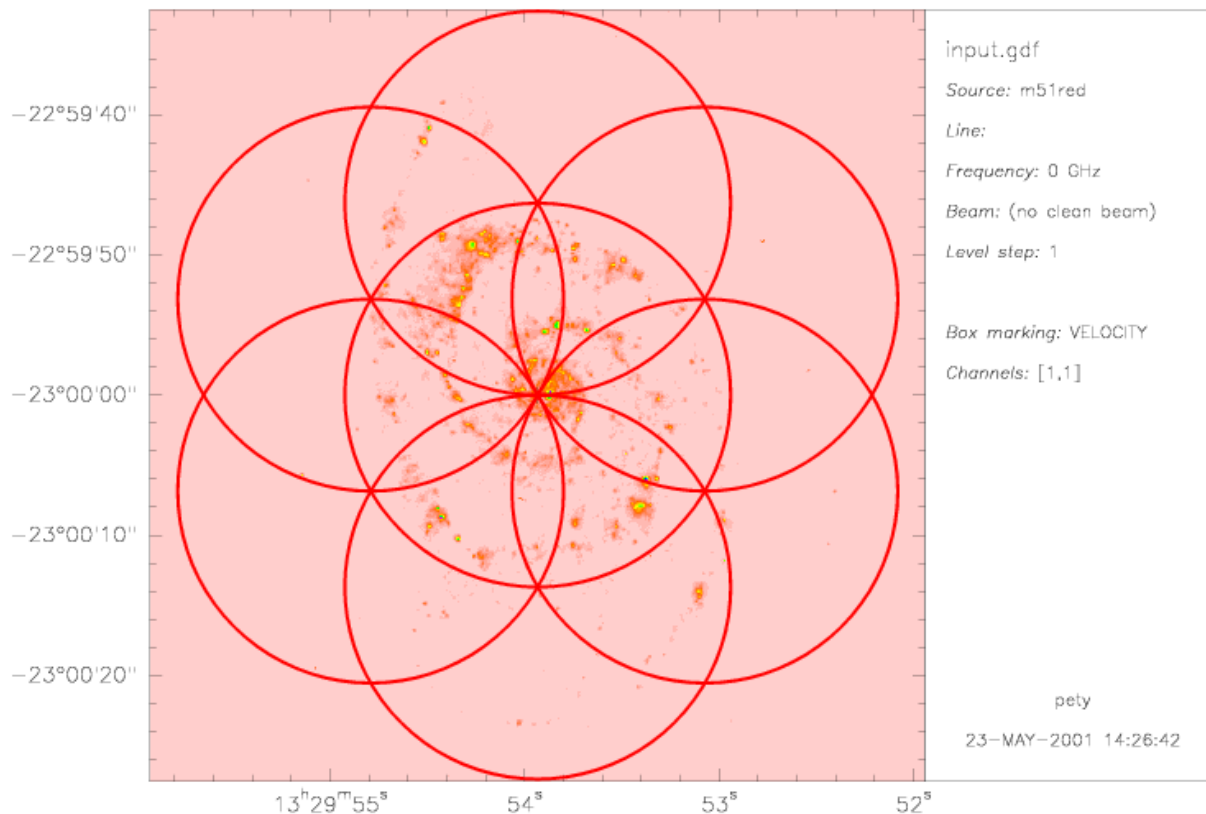
Type of simulations

- Single-dish and/or interferometry.
- Single-field or mosaicking.
- ALMA and/or ACA.

Basic Inputs: I. Generalities

- Source model (e.g. an image of the brightness temperature) with astronomical coordinates.
- Observing frequency.
- Source size ⇒ Number and positions of observed fields are automatically found.
- Hour angle to be observed.
- Array configuration.
- Type of simulations: ALMA only, ACA only, ALMA+ACA, ALMA+SD, ACA+SD, ALMA+ACA+SD.

Basic Inputs: II. Example

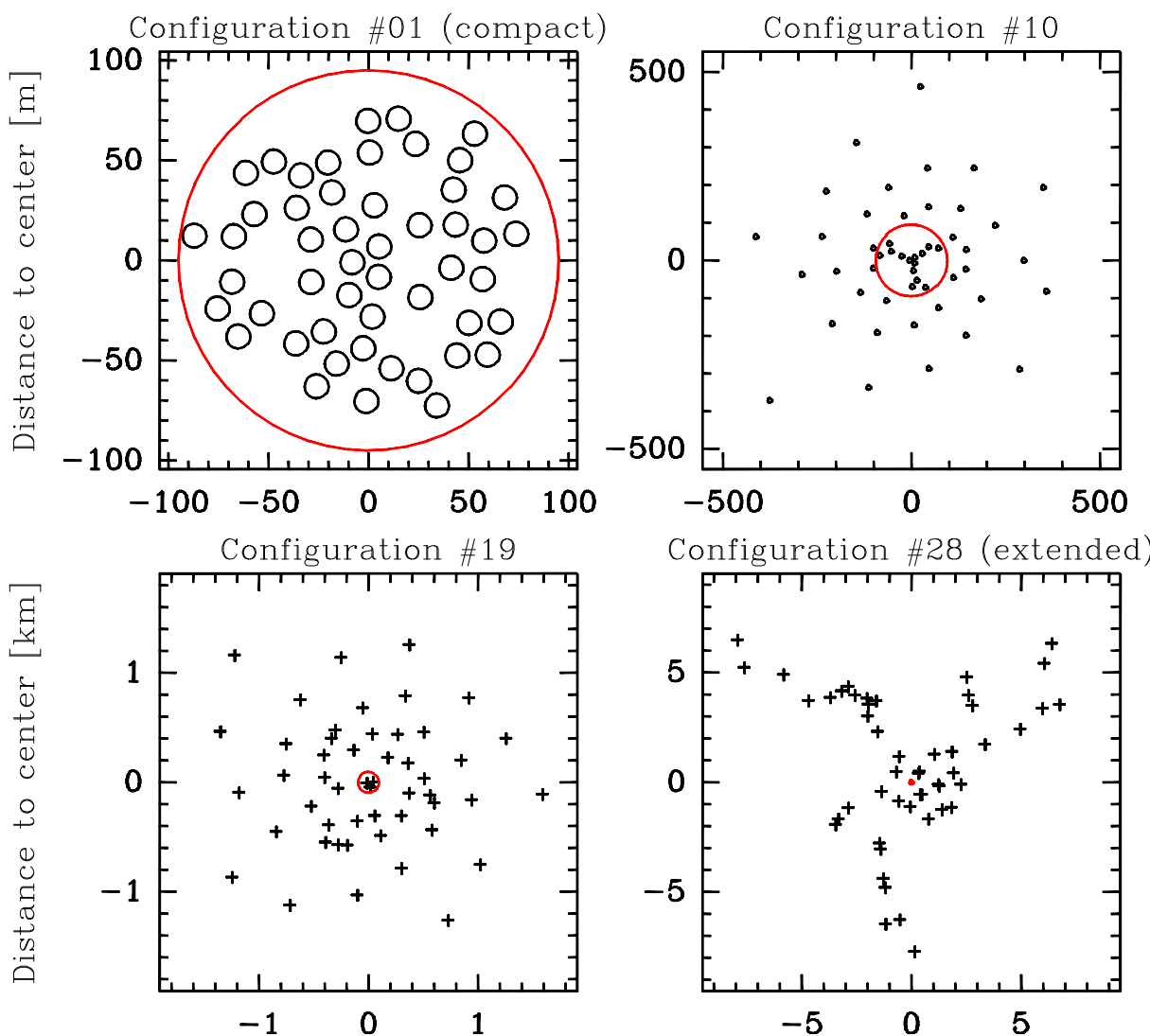


Model image M51 in H α (Structure at every scales).

Type of observation

- 7 field mosaic at 230 GHz.
- Same hexagonal pattern for ALMA and ACA
⇒ oversampled mosaic for ACA.
- Snapshot:
 - 0.3 hour for ALMA;
 - 1.2 hour for ACA and SD.

Basic Inputs: III. Configurations



Updated in 2010

Thanks to F. Levrier (with help from J. Pety, I. Heywood, A. Wootten and K.-I. Morita).

ALMA

- 28 configurations.
- Diameters from 190 m to 18 km.

ACA

- 2 extremely compact configurations.
- One stretched north-south to avoid shadowing.

Bird eye view similar to Nazca lines



Ideal Simulation

Simulation of interferometric observations $V(u, v) = \text{FFT} \{B_{\text{prim}} \cdot I_{\text{source}}\}(u, v)$
Time $\Rightarrow uv$ coverage \Rightarrow Sampling of $\text{FFT} \{B_{\text{prim}} \cdot I_{\text{source}}\}$.

For wide-field imaging

- Simulation of On-The-Fly single-dish observations: $I_{\text{sd}} = B_{\text{sd}} * I_{\text{source}}$.
- Computation of pseudo-visibilities from single-dish observations.
- Merging of pseudo-visibilities and interferometric visibilities.

Imaging and deconvolution

Comparison between simulated result and original image

Image plane comparison: I. ALMA only

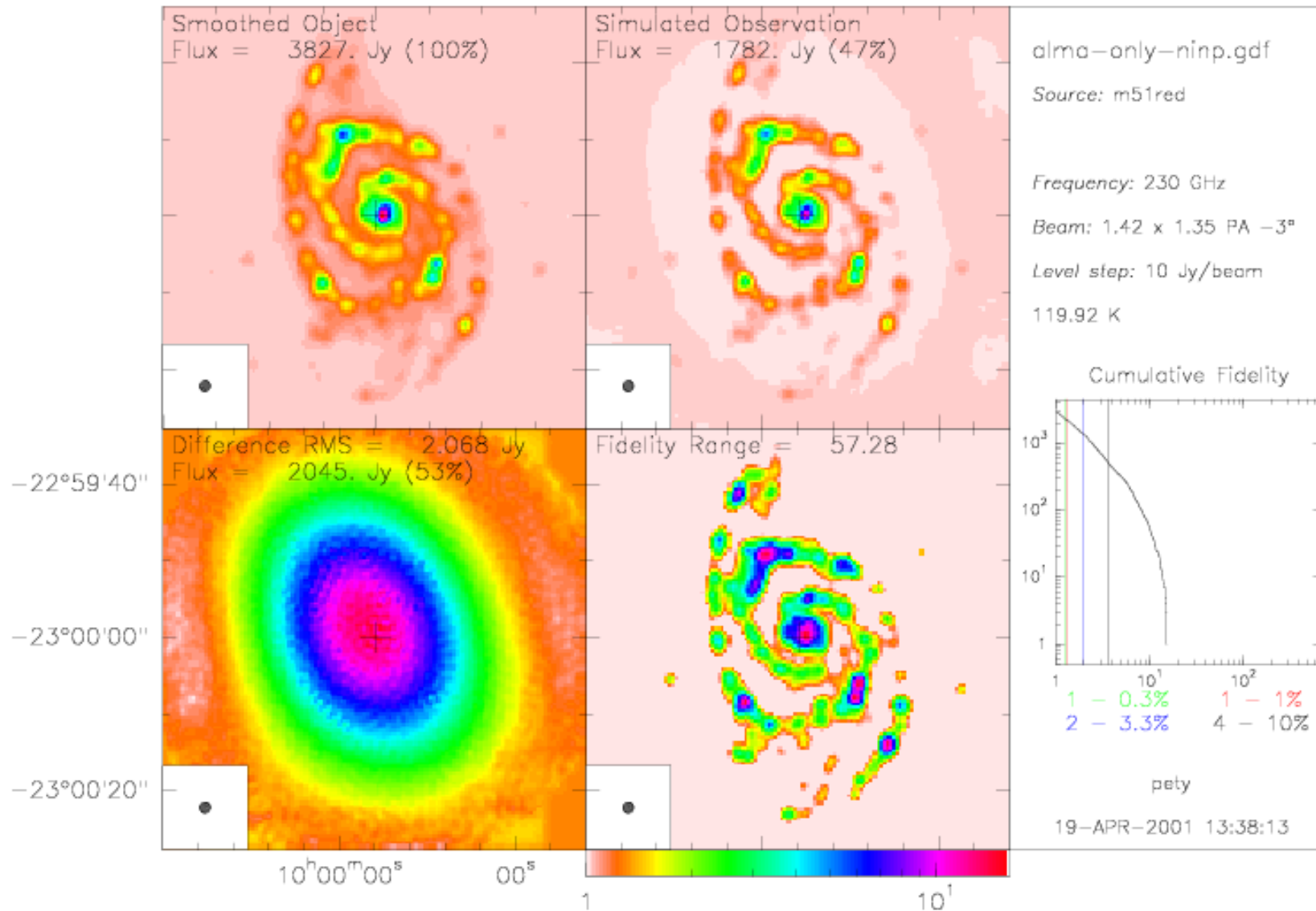


Image plane comparison: II. ALMA + SD

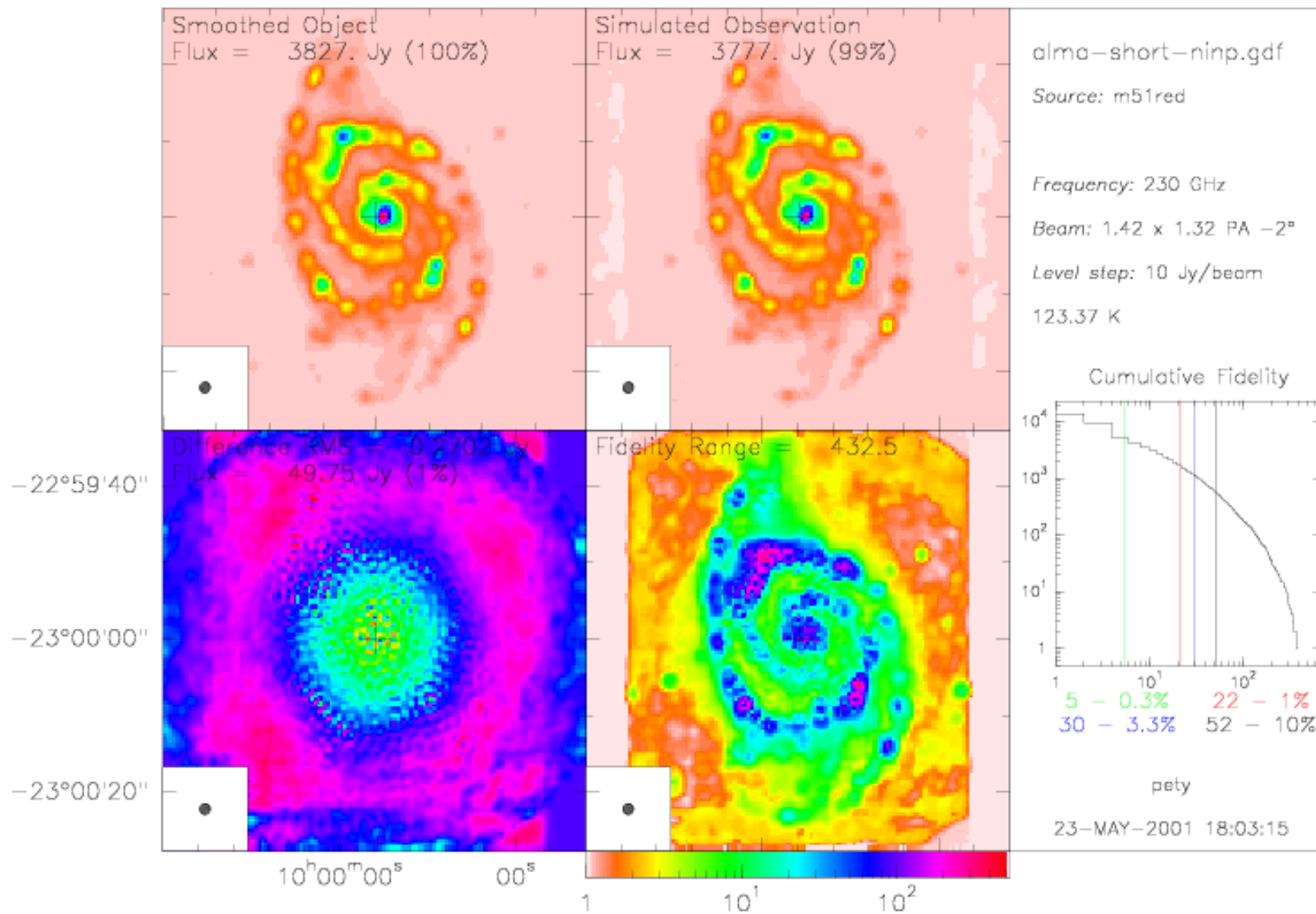
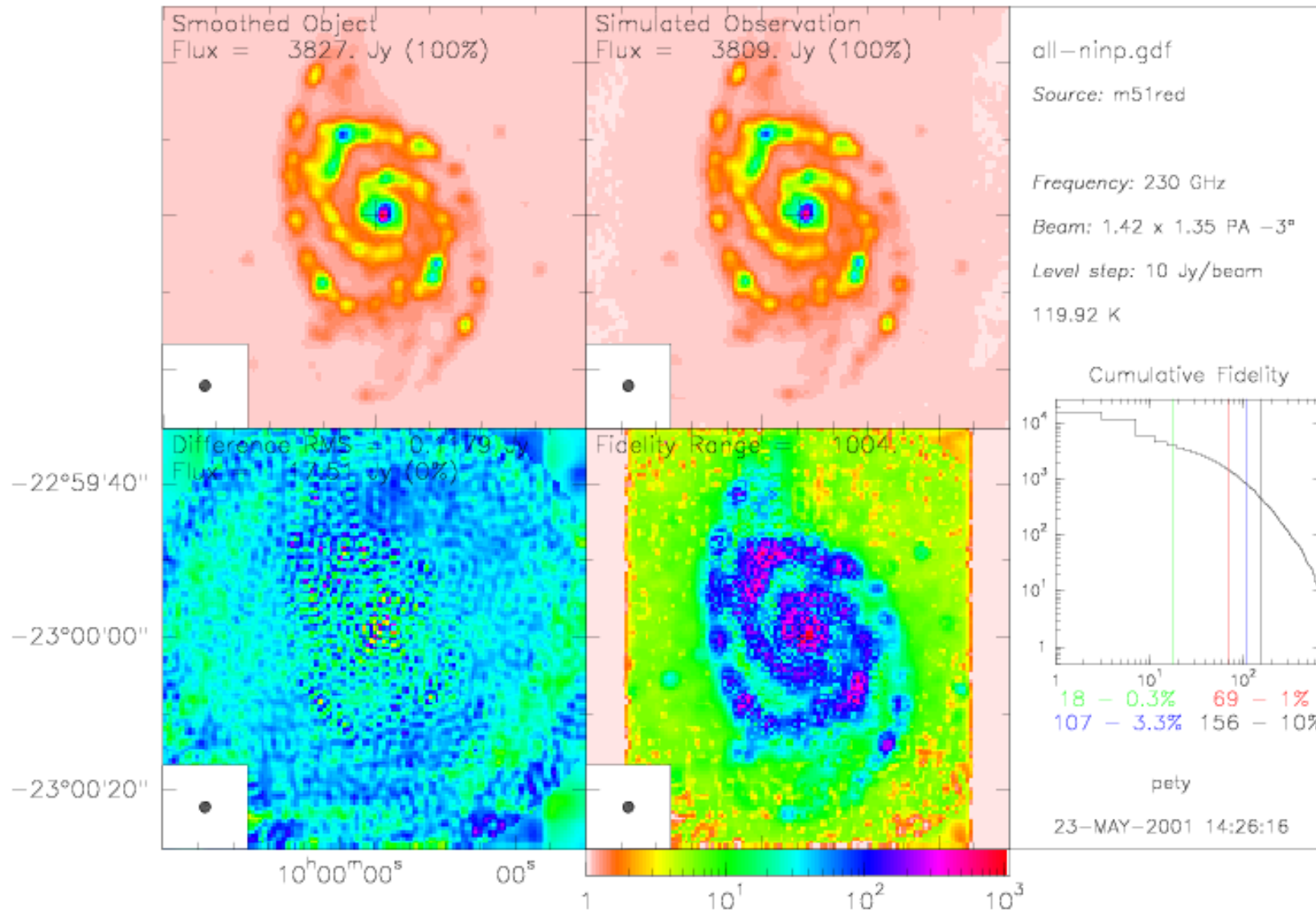
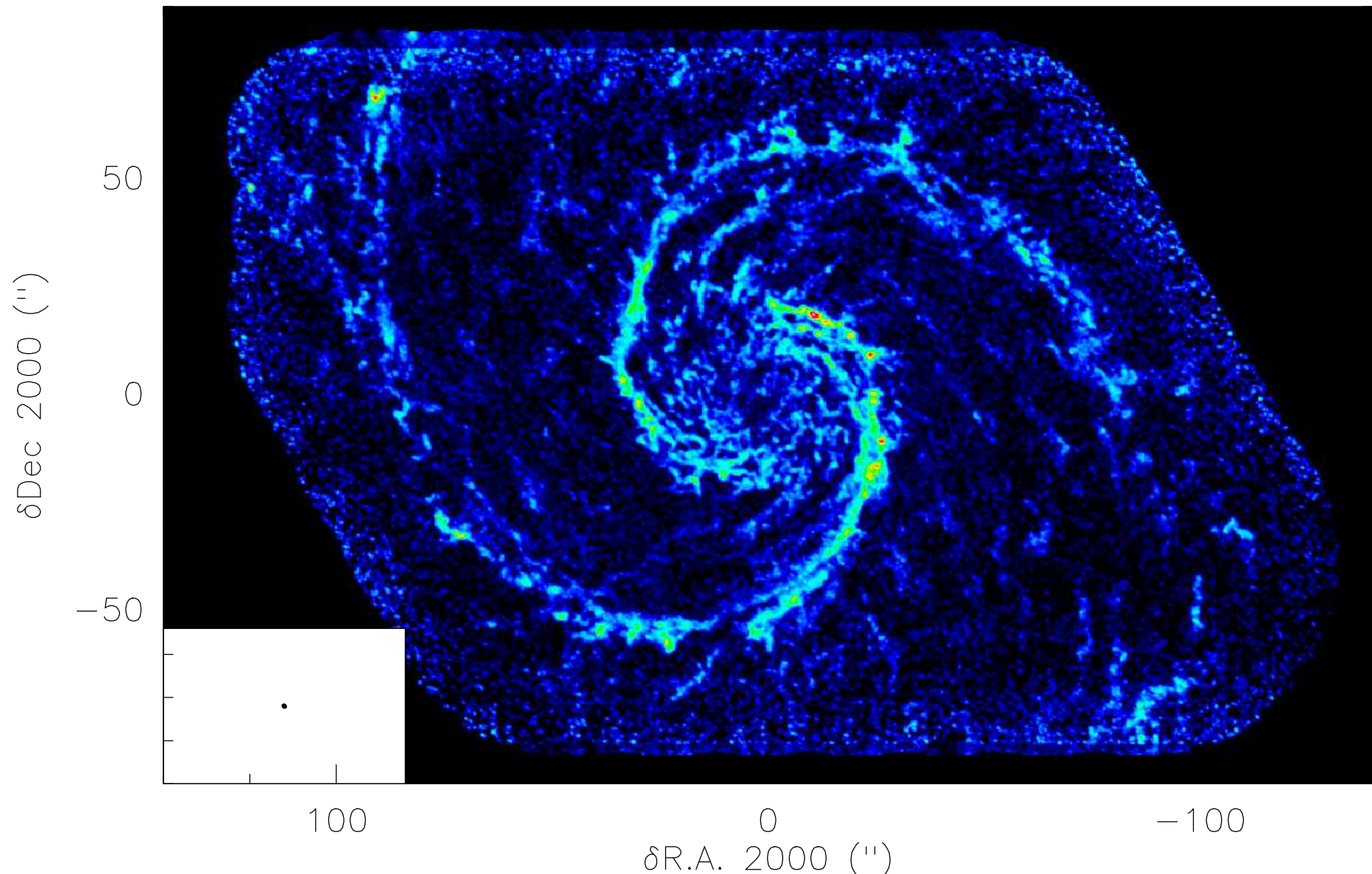


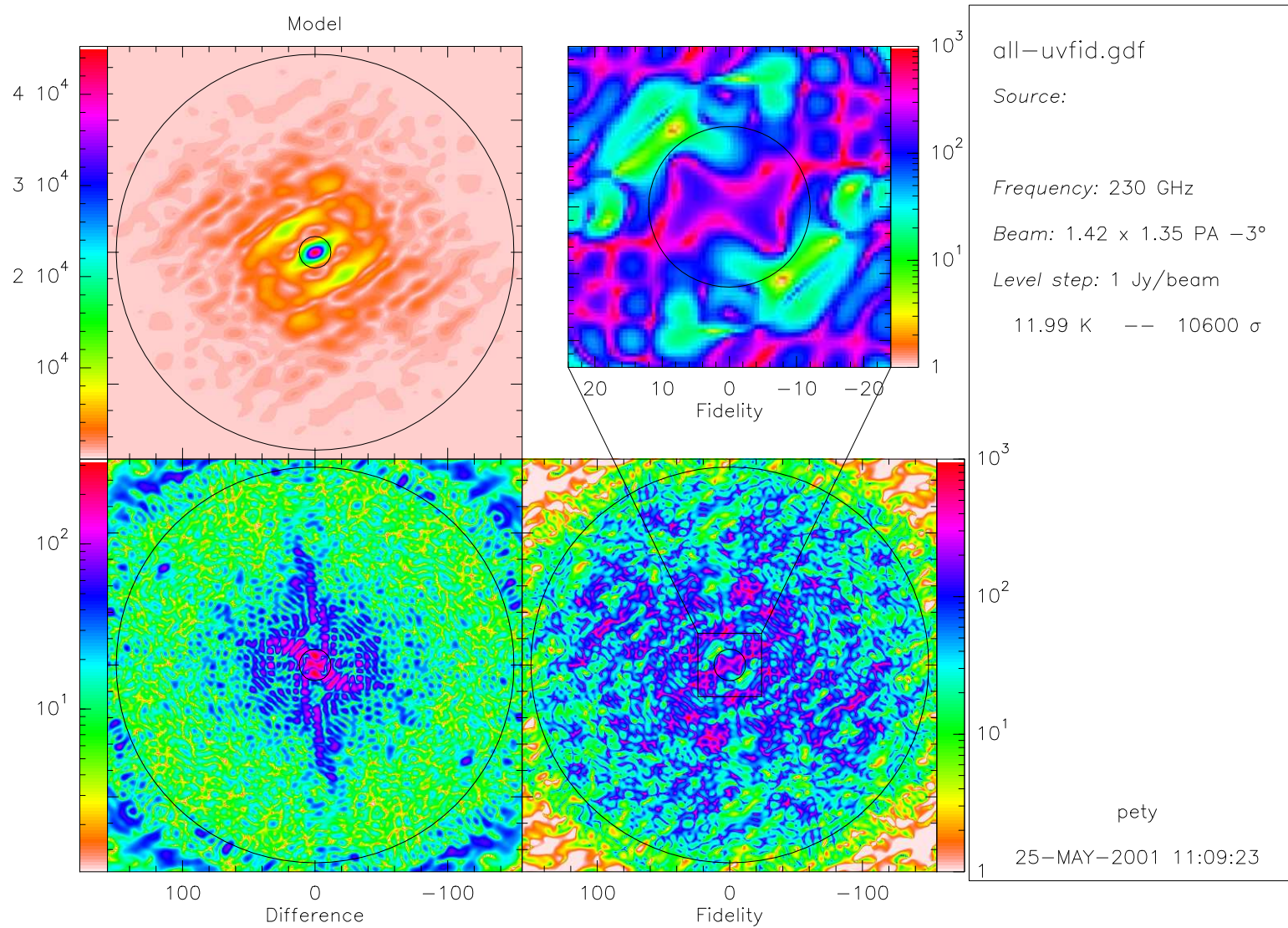
Image plane comparison: III. ALMA + ACA + SD



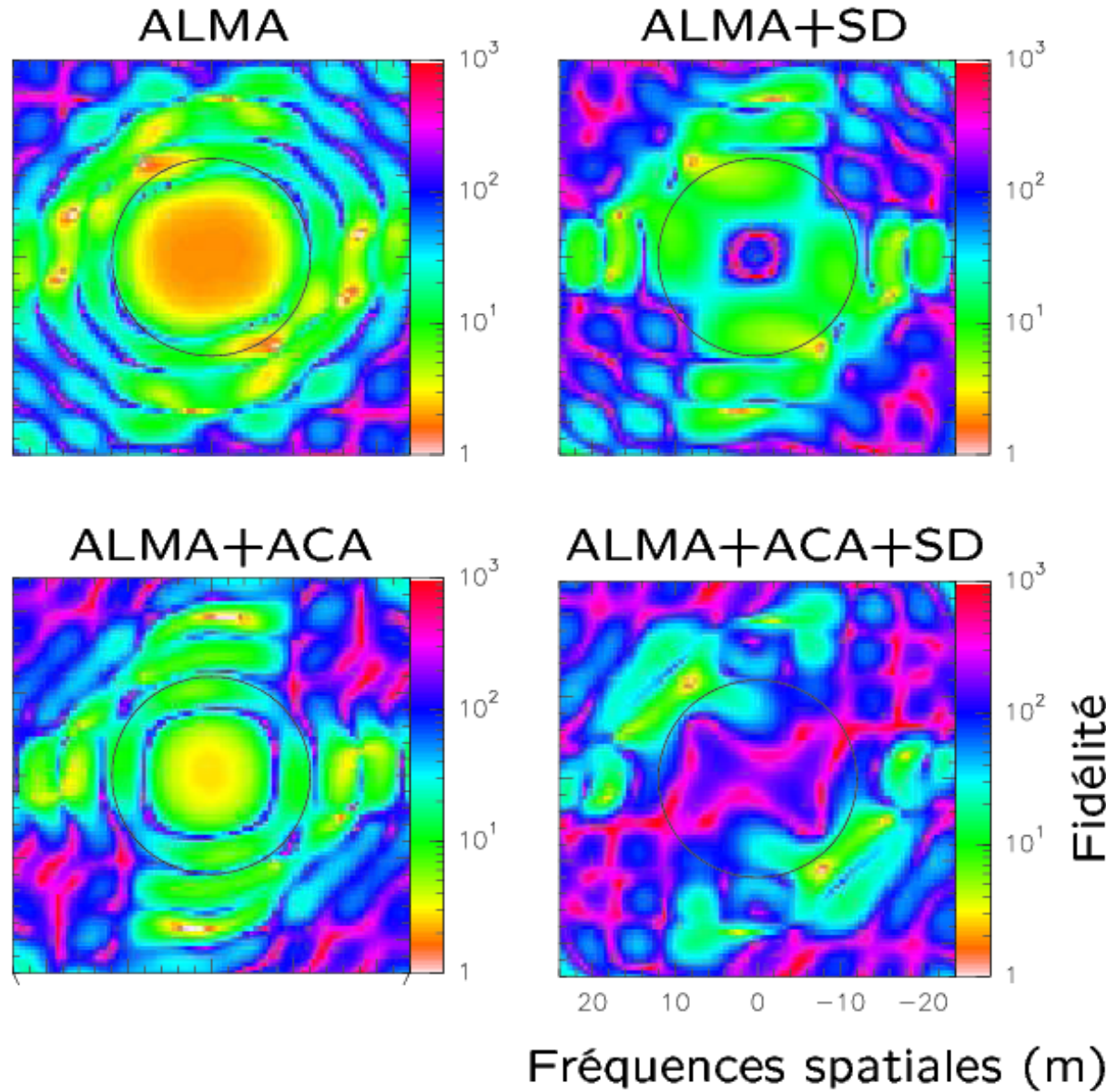
Parenthesis: M51 as seen by PdBI+30m in ^{12}CO ($J=1-0$)
(Schinnerer and the PAWS team)



uv plane comparison: I. ALMA + ACA + SD



uv plane comparison: II. Which part measures what?



Deconvolving Data from an Heterogeneous Array

I. Joint Deconvolution

1. FFT and construction of 2 dirty mosaics (ALMA and ACA+SD):

$$J = \sum_i \frac{B_i}{\sigma_i^2} F_i \left/ \sum_i \frac{B_i^2}{\sigma_i^2} \right. \quad \text{with } \begin{cases} B_i \text{ primary beams} \\ F_i \text{ dirty maps} \end{cases} ;$$

2. Selection of mosaic with highest SNR;

3. Search of clean components using:

- CLARK algorithm if using the ALMA image;
- SDI algorithm if using the ACA image;

4. Careful removing of found components from both images (always beginning with the ALMA image);

5. Choice of the image with the highest residual SNR to be the next one to work with and go to point 3;

6. Weighting of CLEAN components by the ALMA clean beam and addition of weighted residuals.

Deconvolving Data from an Heterogeneous Array

II. Hybridization in the uv Plane

Method

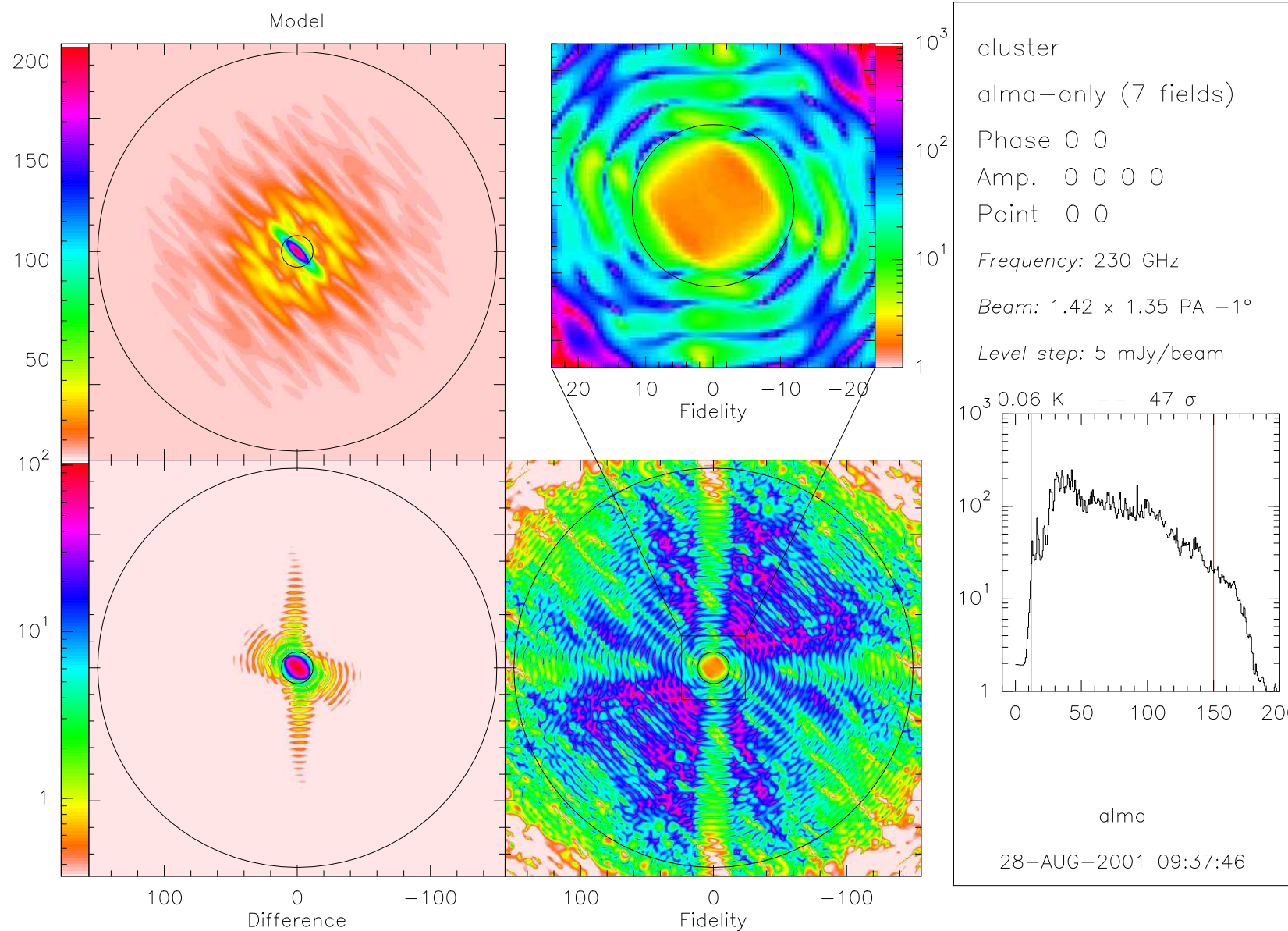
1. Deconvolution of ALMA+SD;
2. Deconvolution of ACA+SD;
3. FFT of the 2 clean images $\Rightarrow \tilde{J}_{\text{ALMA}}$ and \tilde{J}_{ACA} ;
4. Linear combination:

$$\tilde{H} \simeq \begin{cases} \tilde{J}_{\text{ALMA}} & \text{for } \sqrt{u^2 + v^2} > 15 \text{ m} \\ \tilde{J}_{\text{ACA}} & \text{for } \sqrt{u^2 + v^2} < 15 \text{ m;} \end{cases}$$

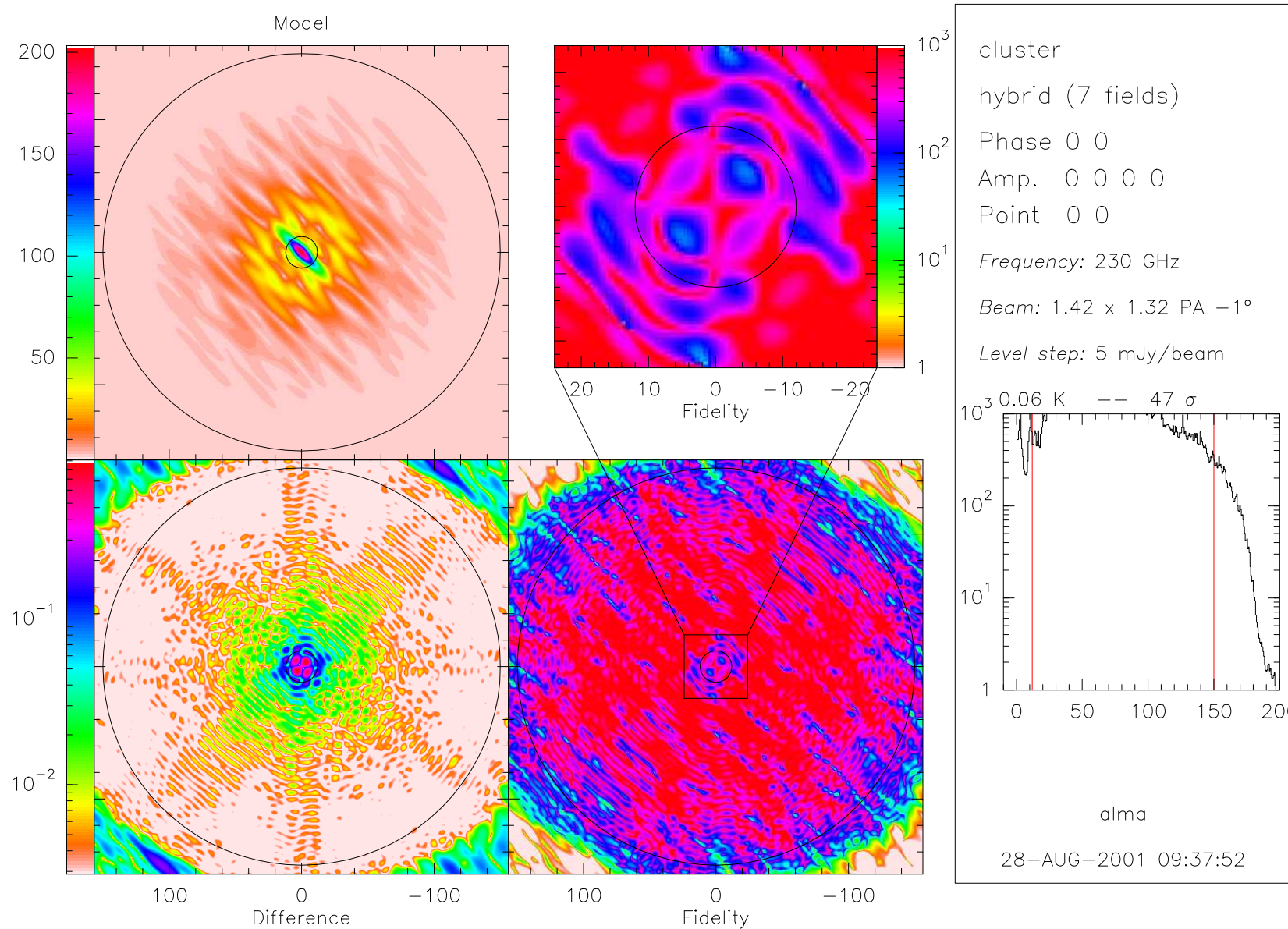
5. Inverse FFT of \tilde{H} .

Advantages Fast, robust and often optimal.

Impact of Single-Dish on deconvolution of long spacings



Impact of Single-Dish on deconvolution of long spacings



More realistic simulations

Simulation of interferometric observations $V(u, v) = \text{FFT} \{B_{\text{prim}}.I_{\text{source}}\}(u, v)$.

Loop between source and calibrator

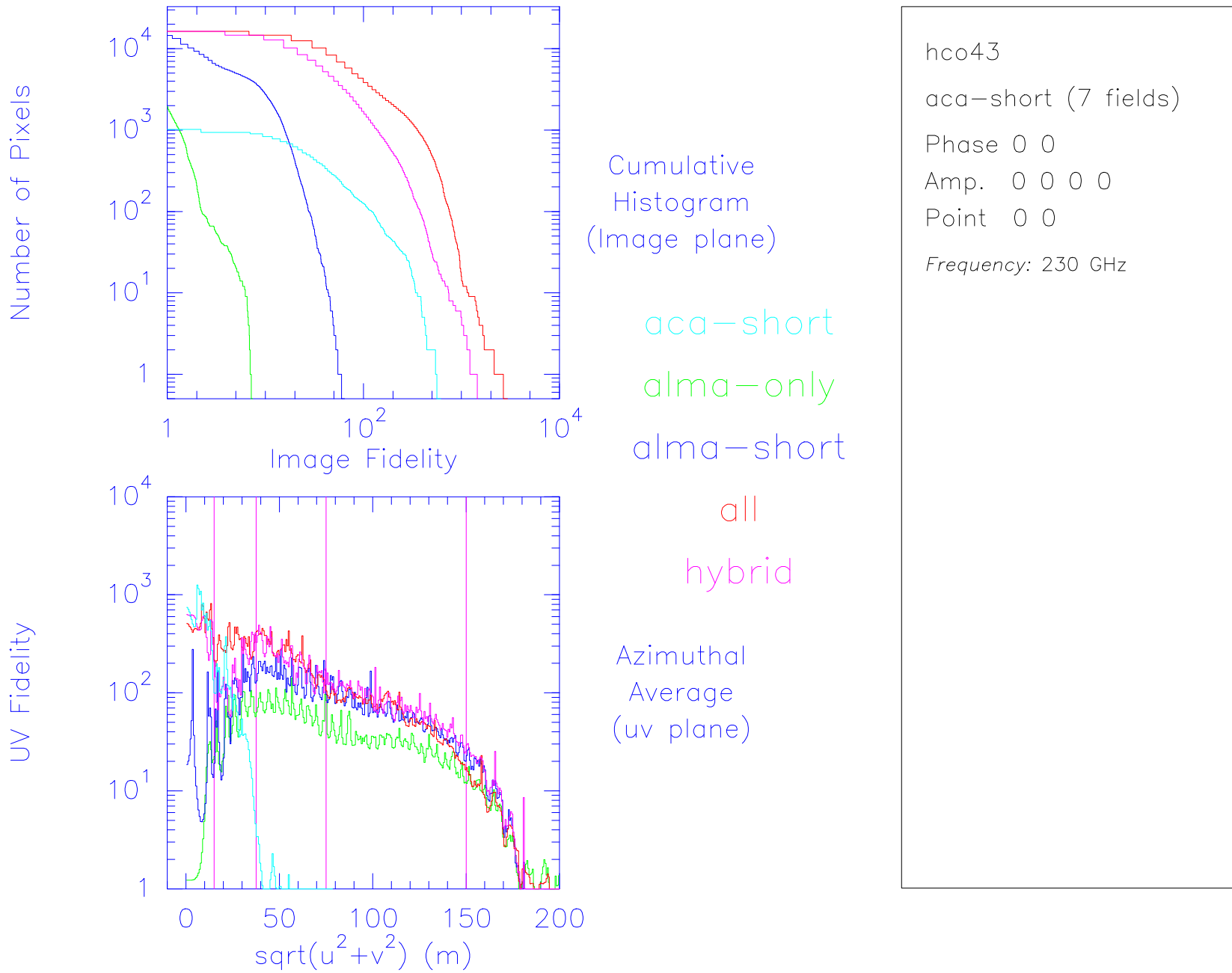
Addition of (simple) errors

- Pointing errors.
- Amplitude calibration errors.
- Thermal noise.
- Phase noise.

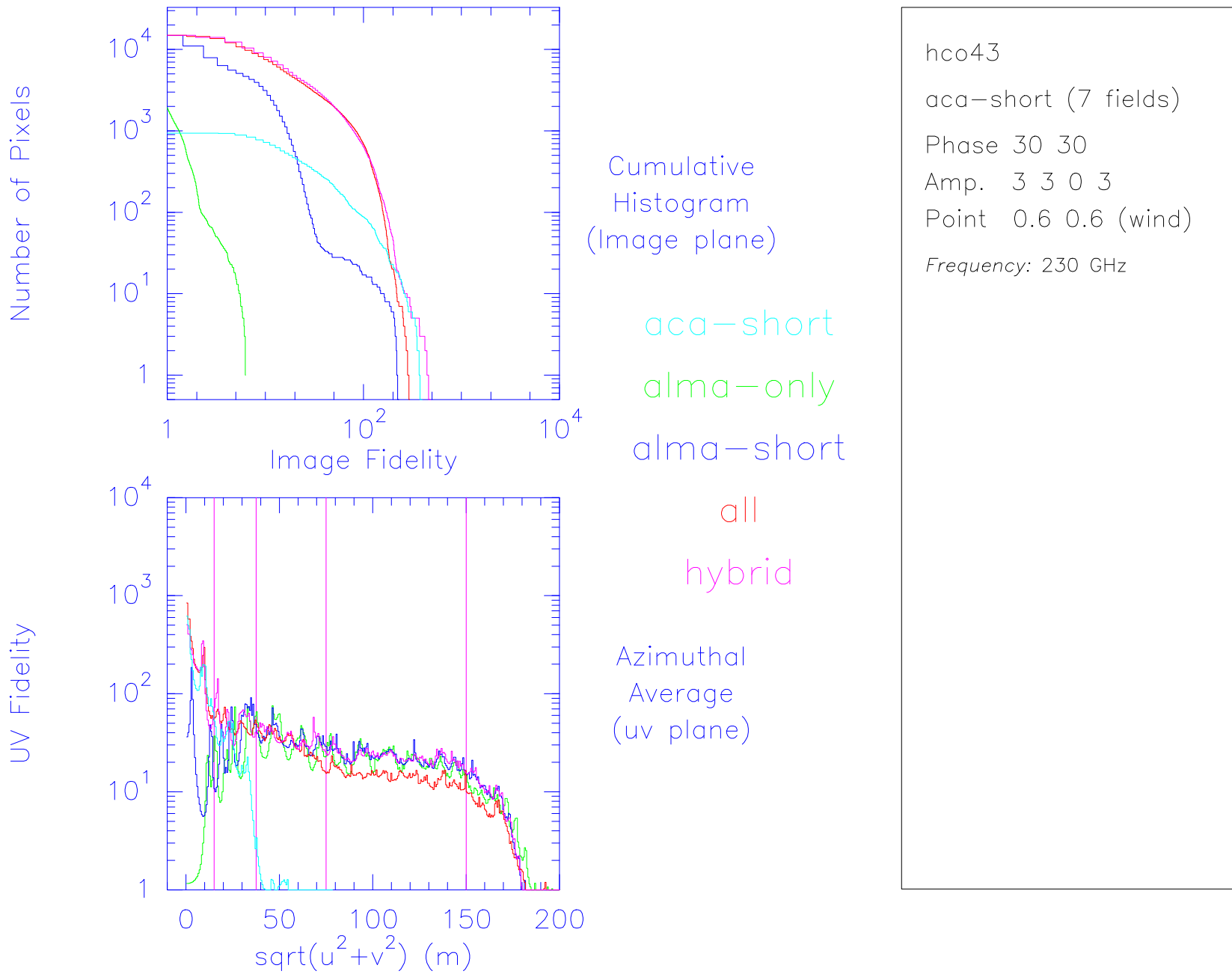
Imaging and deconvolution

Comparison between simulated result and original image

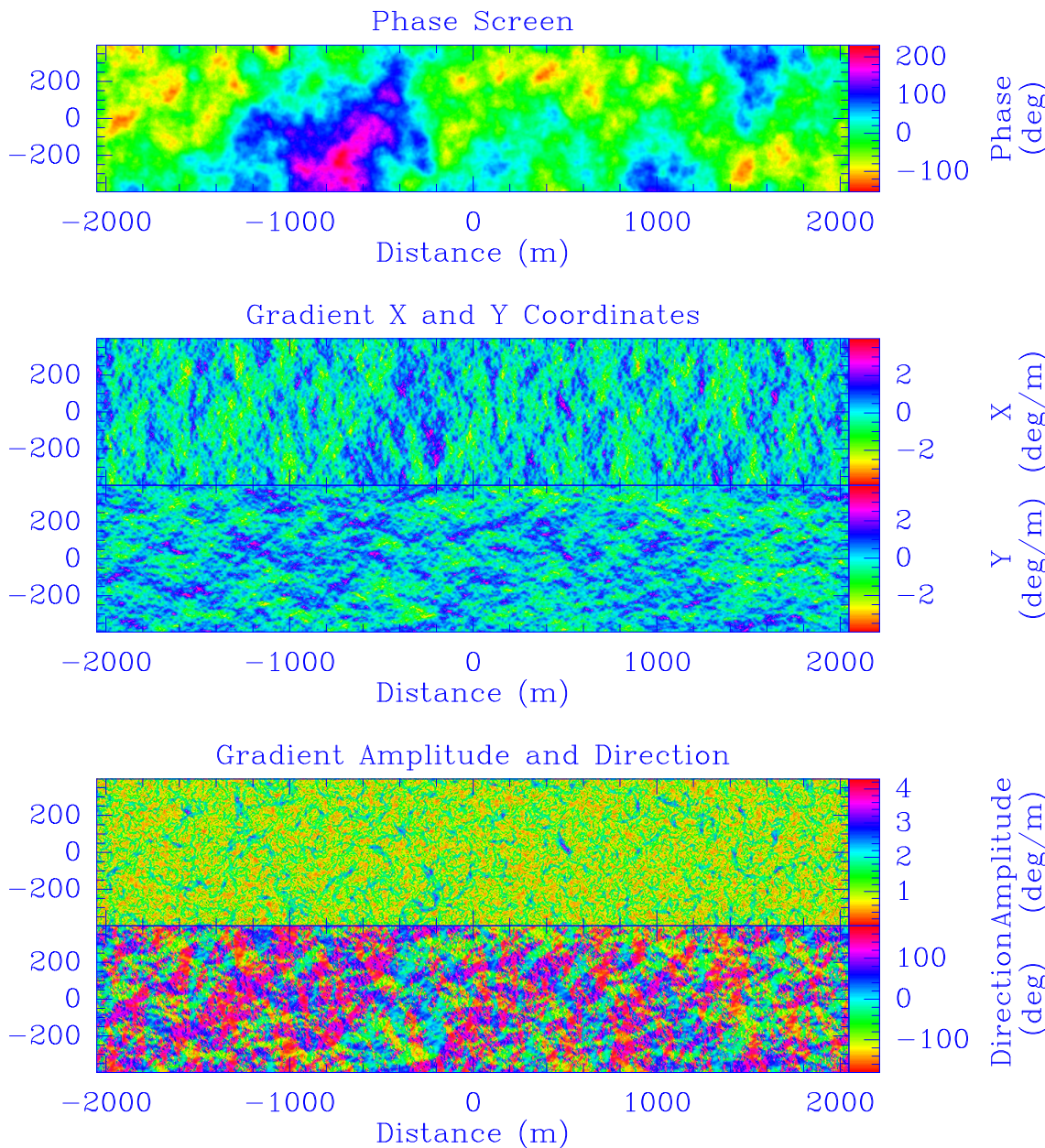
Is it worth the effort? I. Ideal Case



Is it worth the effort? II. Typical Case



Atmospheric phase model



Phase noise

- 2-D screen generated in the Fourier plane.
- Scaled according to input phase at 300 m.
- Elevation dependency $\propto \sqrt{\text{Airmass}}$.
- Move above ALMA during the observations, with a given speed and direction.
- Consistent source/calibrators phase noise.

Dynamic (anomalous) refraction

- Proportional to gradient of phase screen.
- Negligible compared to direct phase noise effect.

Phase calibration

Standard calibration Spline fit through the calibrator data (PdBI method).

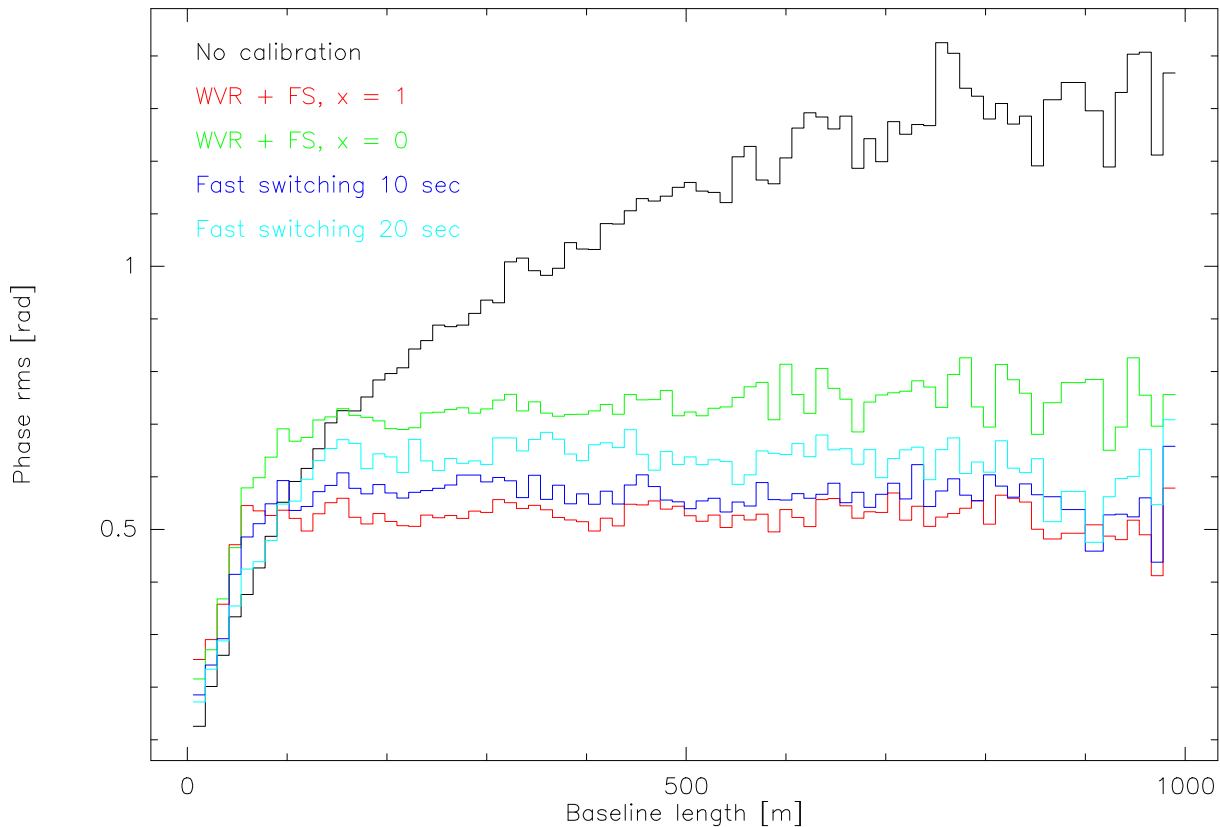
Fast switching (FS) Linear interpolation of the phase between two consecutive calibrator measurements.

Water Vapor Radiometry (WVR)

- Real time phase correction based on water vapor measurements.
- Corrected phase modeled as $P_{\text{WVR}}(t) = P(0) + \chi(P(t) - P(0)) + N(t)$
- Still need a subsequent phase calibration.

WVR + FS A WVR is used and an offset is removed from the last calibration.

Comparison of Phase Calibration Schemes

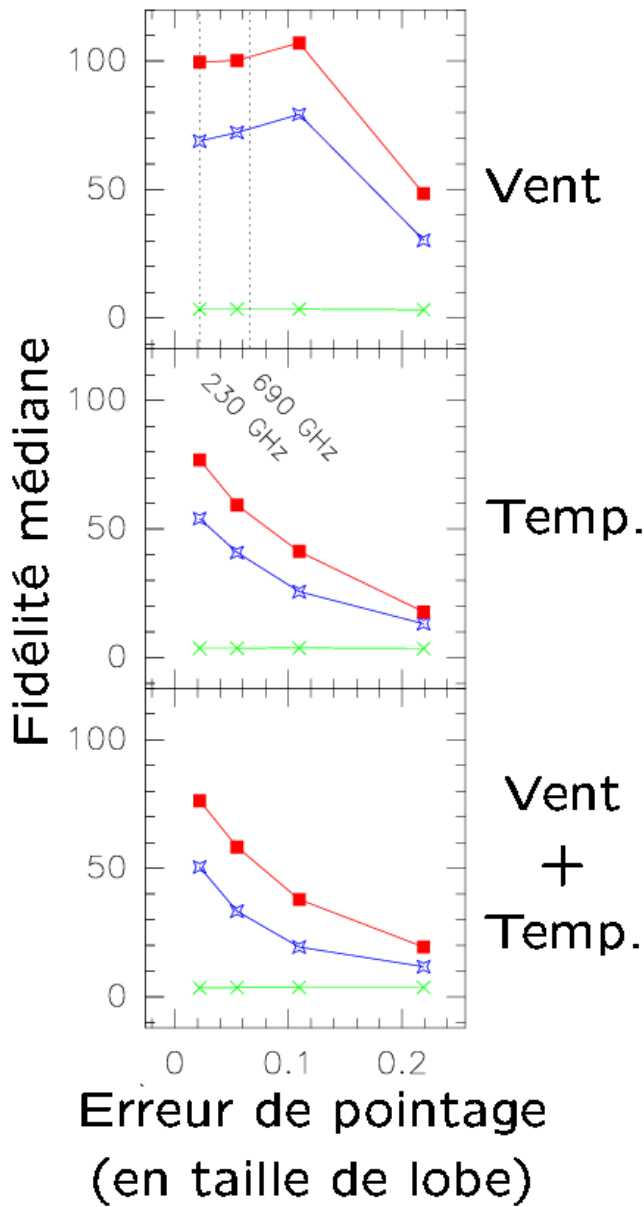


Legend

- No calibration;
- Offset correction every 20 seconds;
- Linear correction every 20 seconds;
- Linear correction every 10 seconds;
- Perfect WVR + offset correction every 20 seconds.

Note Calibration adds phase noise at small scales.

Pointing errors



Wind

- Random within direction and magnitude range.
- Shallow correlation between antennas (50%).
- Timescale \sim second.

Temperature

- Slow drift with time between 2 calibrations.
- Strong correlation between antennas (70%).
- Timescale \sim a few minutes.

Color scheme

- ALMA
- ALMA+SD
- ALMA+ACA+SD

ACA \Rightarrow median fidelity increased by 50-100%.

Bibliography: I. ALMA/ACA Imaging study

ALMA+ACA simulation tool Pety, Gueth & Guilloteau, ALMA memo # 386.

ALMA+ACA simulation results Pety, Gueth & Guilloteau, ALMA memo # 387.

Impact of ACA on the wide-field imaging capabilities of ALMA Pety, Gueth & Guilloteau, ALMA memo # 398.

Wide-field imaging of ALA with the ACA: Imaging simulations Tsutsumi, Morita, Hasegawa & Pety, ALMA memo # 488.

Bibliography: II. Scientific papers

Detecting Planets in Protoplanetary Disks: A Prospective Study S. Wolf et al. 2002,
ApJ, 566, L97.

Large-Scale Vortices in Protoplanetary Disks: On the Observability of Possible Early Signs
S. Wolf & H. Klahr, ApJ, 578, L79.

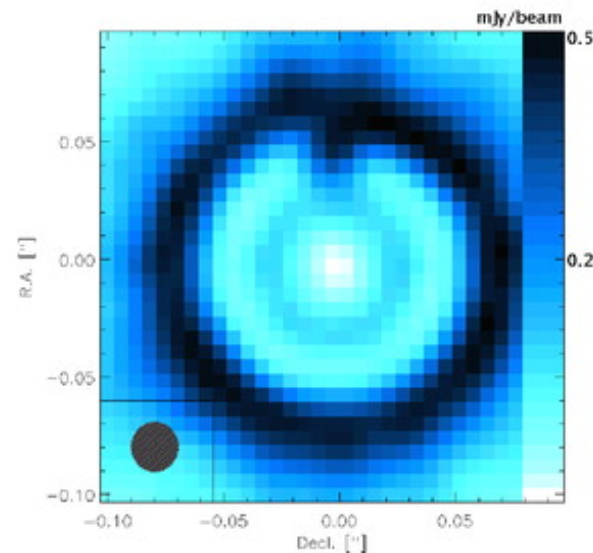
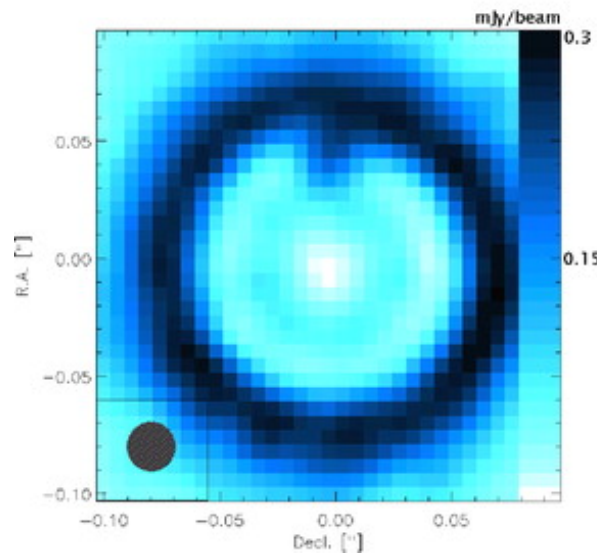
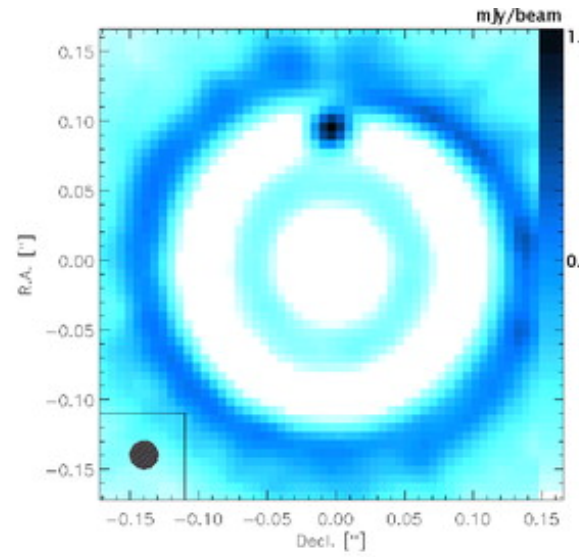
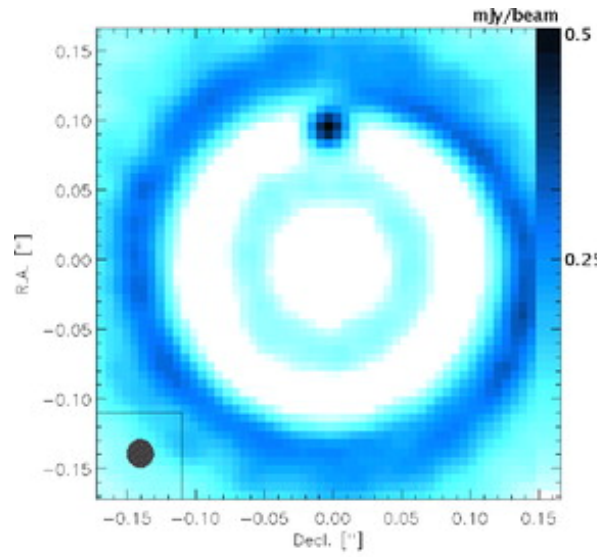
On the Observability of Giant Protoplanets in Circumstellar Disks S. Wolf & G. D'Angelo
2005, ApJ, 619, 1114.

Chemical and Thermal Structure of Protoplanetary Disks as Observed with ALMA
D. Semenov et al. 2008, ApJ, 673, L195.

Early stages of star formation: The ALMA promise P. André et al. 2008, *Astrophys. Space Sci.*, 313, 29.

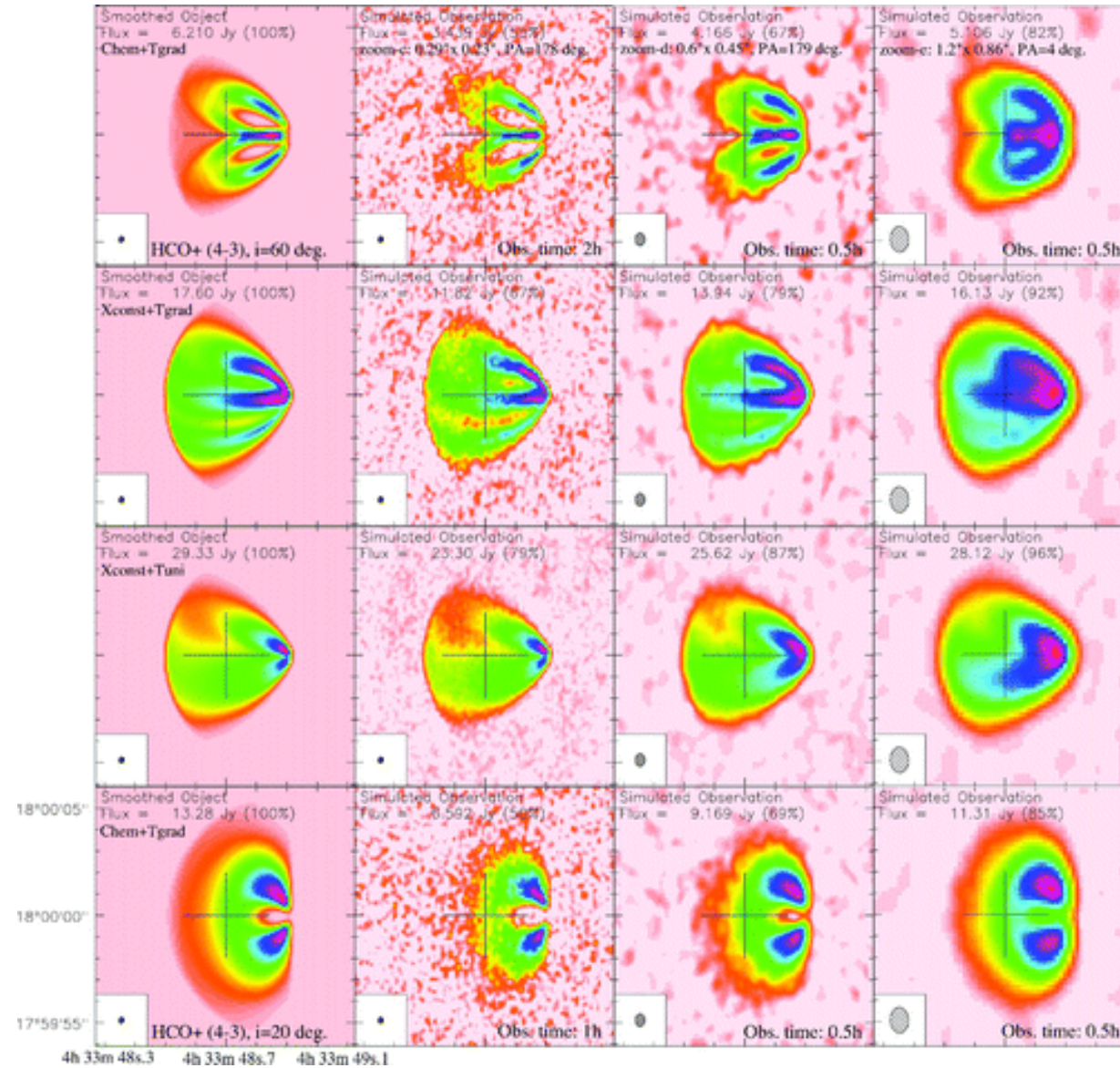
Physical studies of Centaurs and trans-Neptunian objects with ALMA Mouillet et al.,
Icarus, submitted.

Scientific Examples: I. On the Observability of Giant Protoplanets in Circumstellar Disks (S. Wolf & G. D'Angelo 2005)



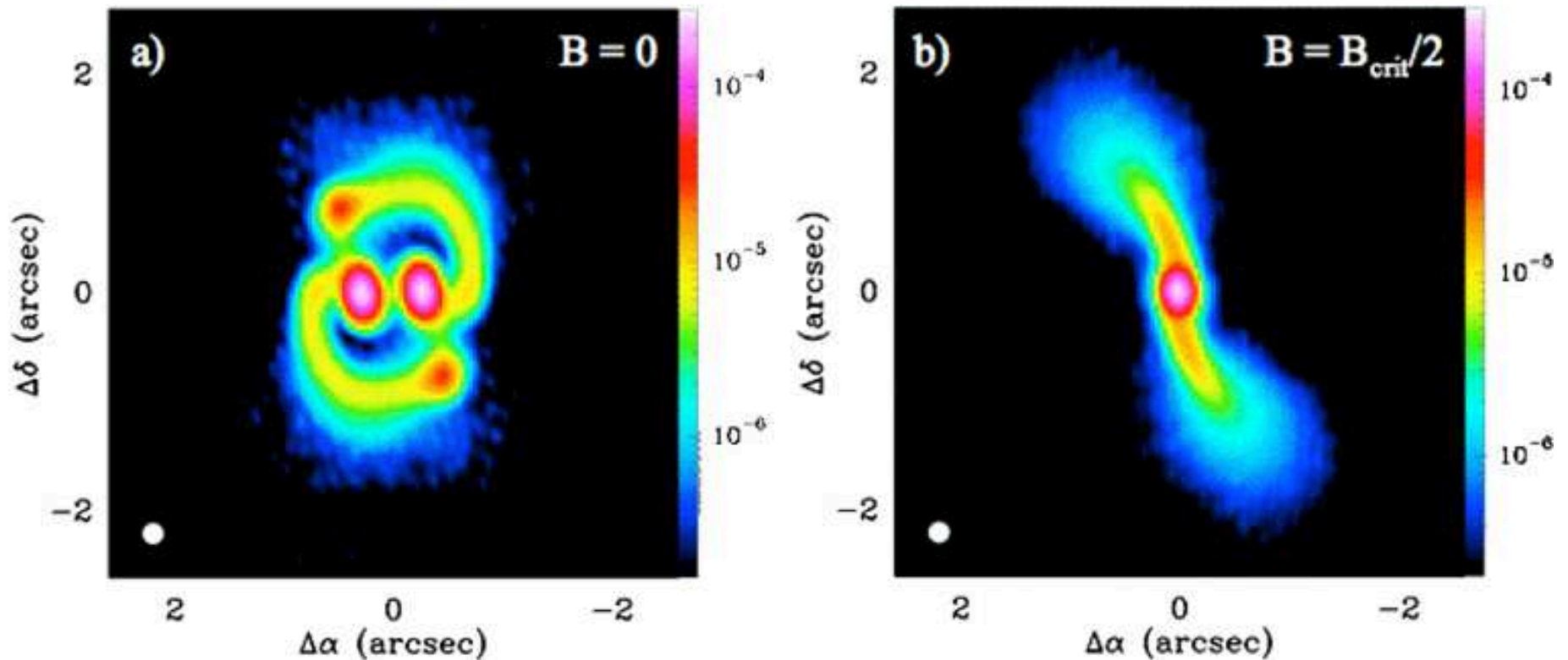
Left $1 M_{\text{Jupiter}}$.
Right $5 M_{\text{Jupiter}}$.
Top At 50 pc.
Bottom at 100 pc.

Scientific Examples: II. Chemical and Thermal Structure of Protoplanetary Disks as Observed with ALMA (D. Semenov et al. 2008)



Line HCO⁺ (4-3).
Rows 4 different chemical models.
Columns Model + 3 different simulations (configurations and/or observing time).

Scientific Examples: III. Early stage of star formation: The ALMA promise (Andre et al. 2008)

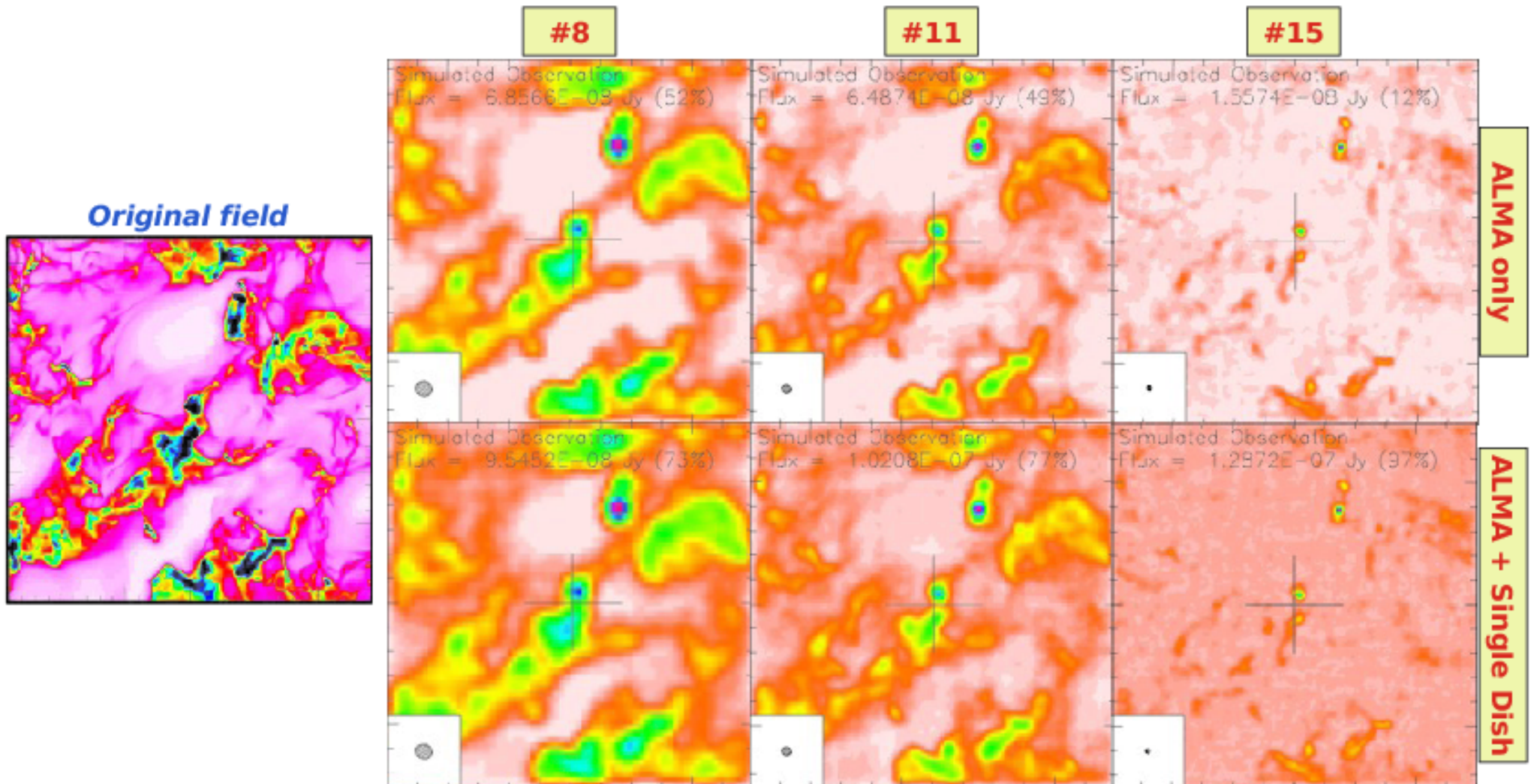


Collapse and fragmentation of a protostellar core MHD simulations from Fromang et al. 2006.

Left $B = 0$.

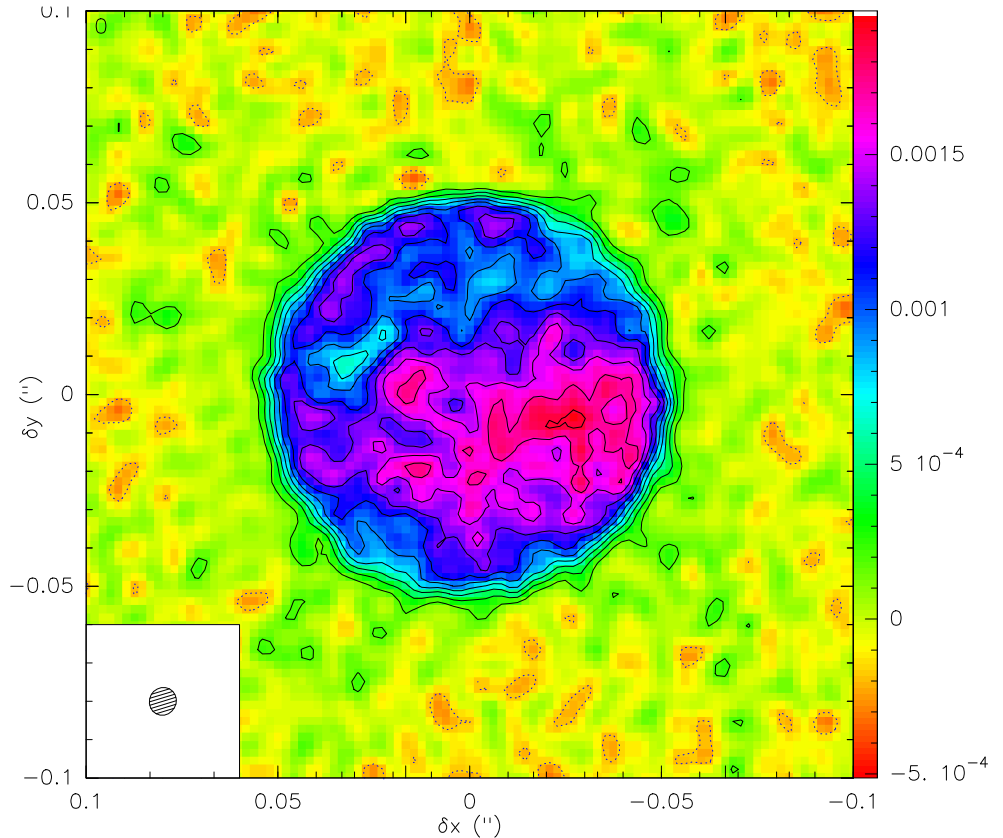
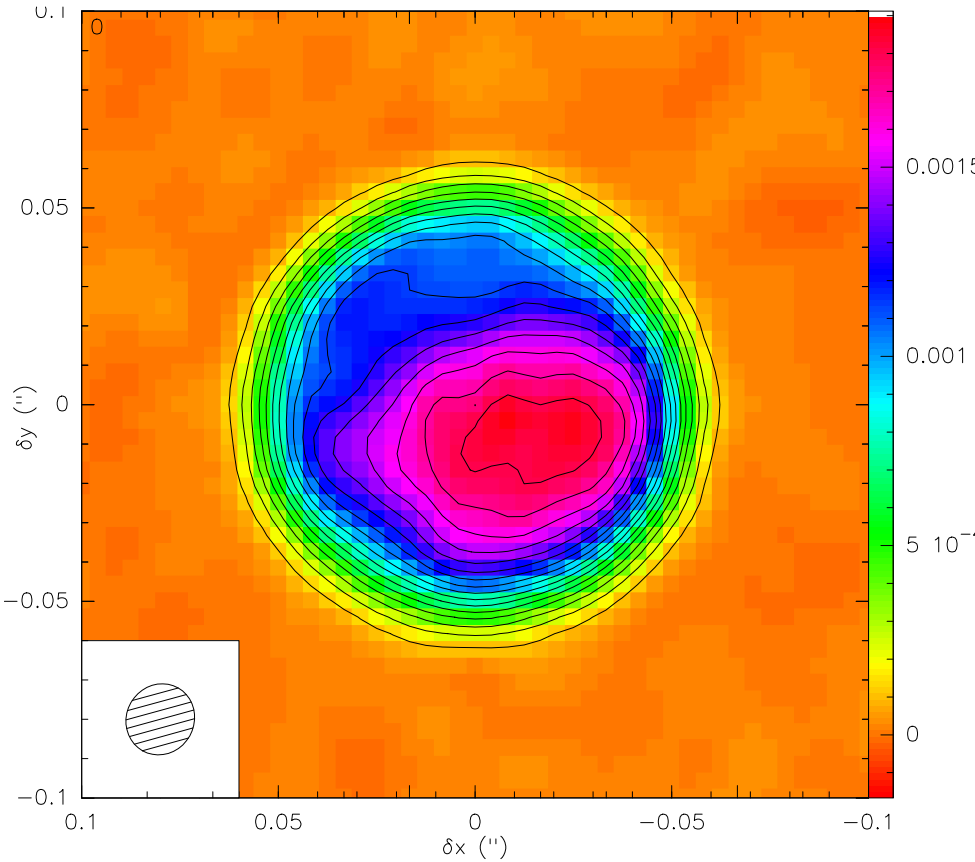
Right $B = 0.5B_{\text{crit}}$.

Scientific Examples: IV. Multi-phase ISM and formation of GMCs (Levrier et al. in prep.)



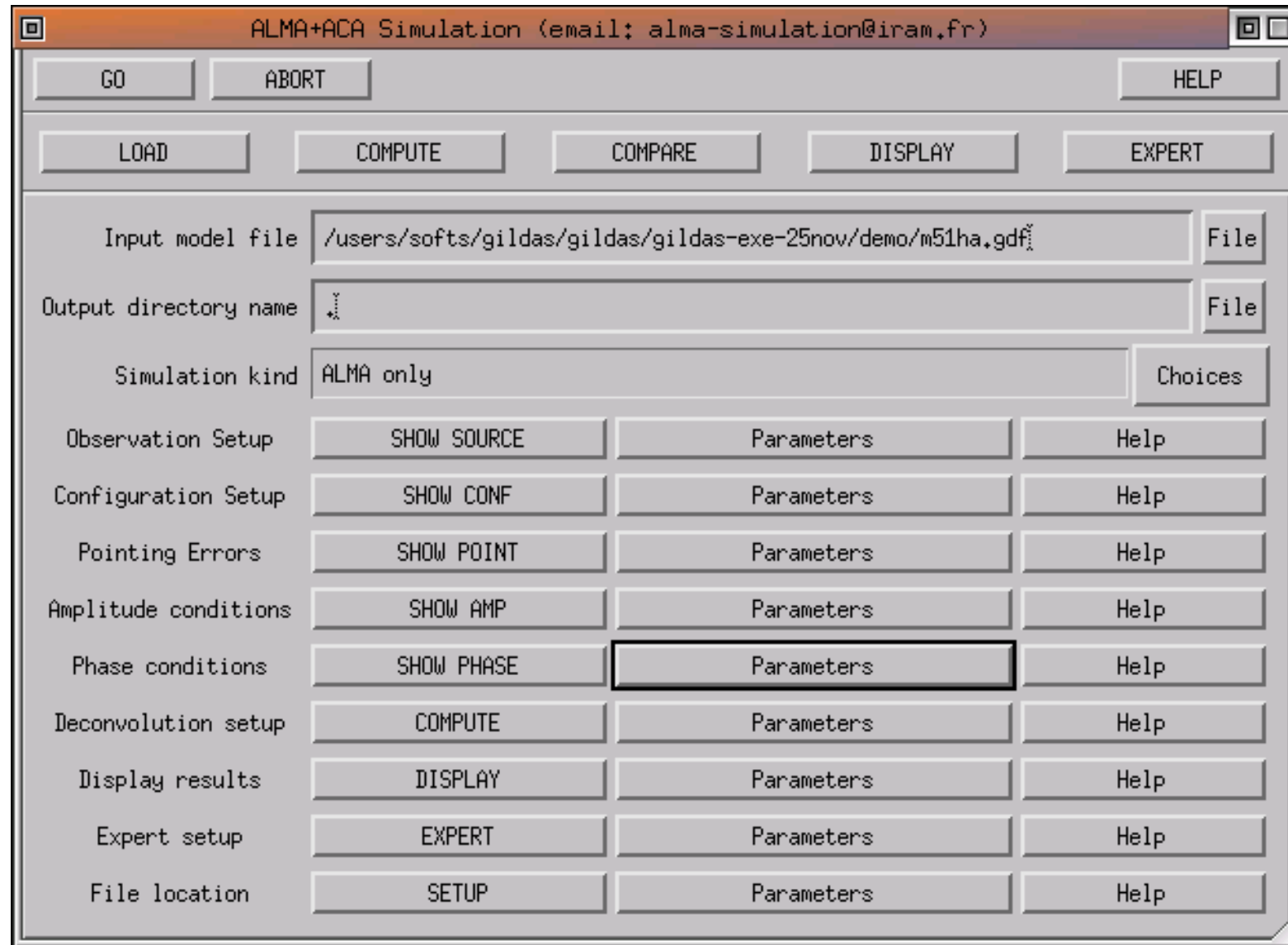
Based on RAMSES simulations of Hennebelle et al.
(part of the ASTRONET STARFORMAT project).

Scientific Examples: V. Physical studies of Centaurs and trans-Neptunian objects with ALMA (Mouillet et al. submitted)

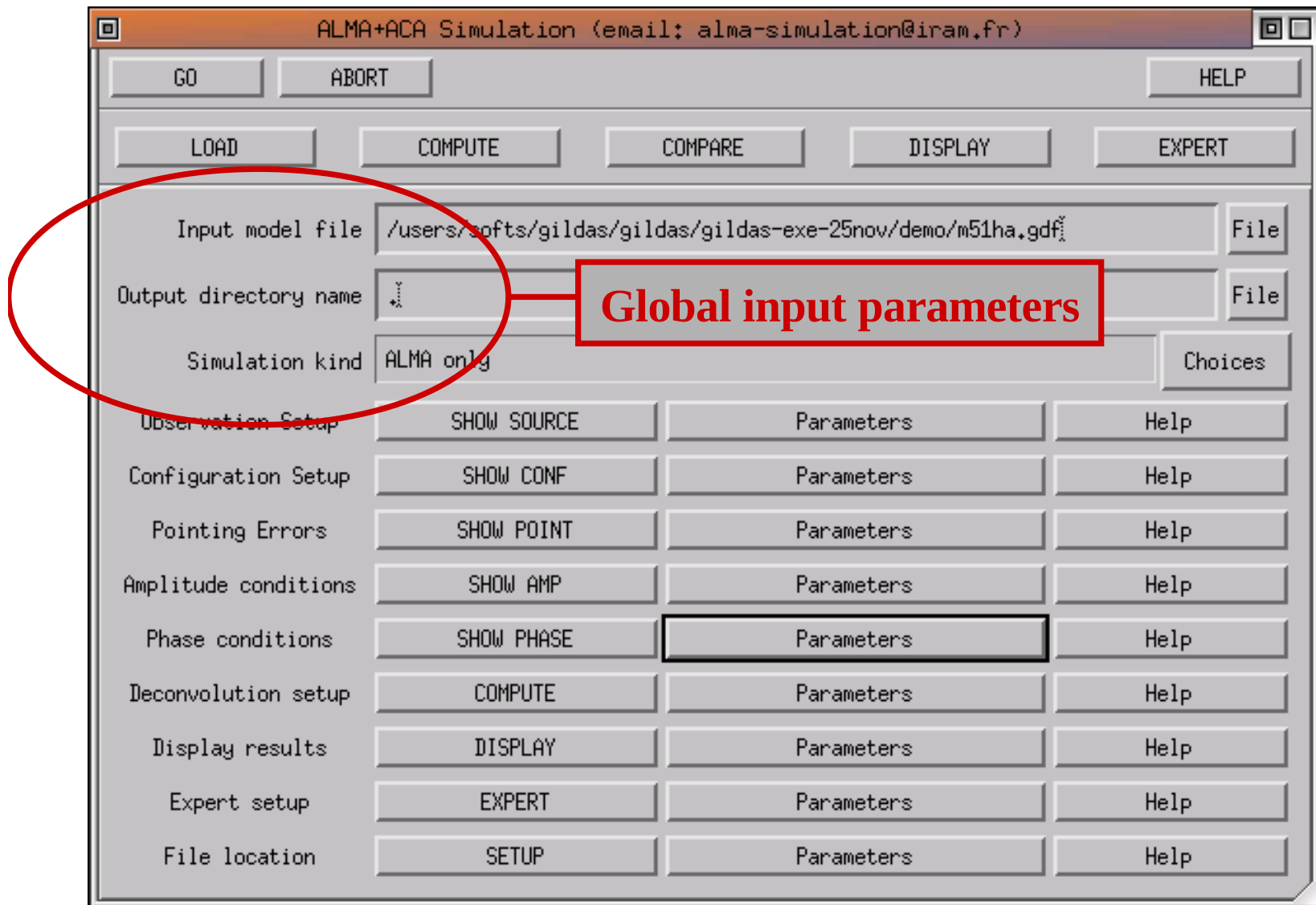


Observations of Pluto during 4 hours (largest baseline: 10 km).
Left: At 345 GHz. Right: At 850 GHz.

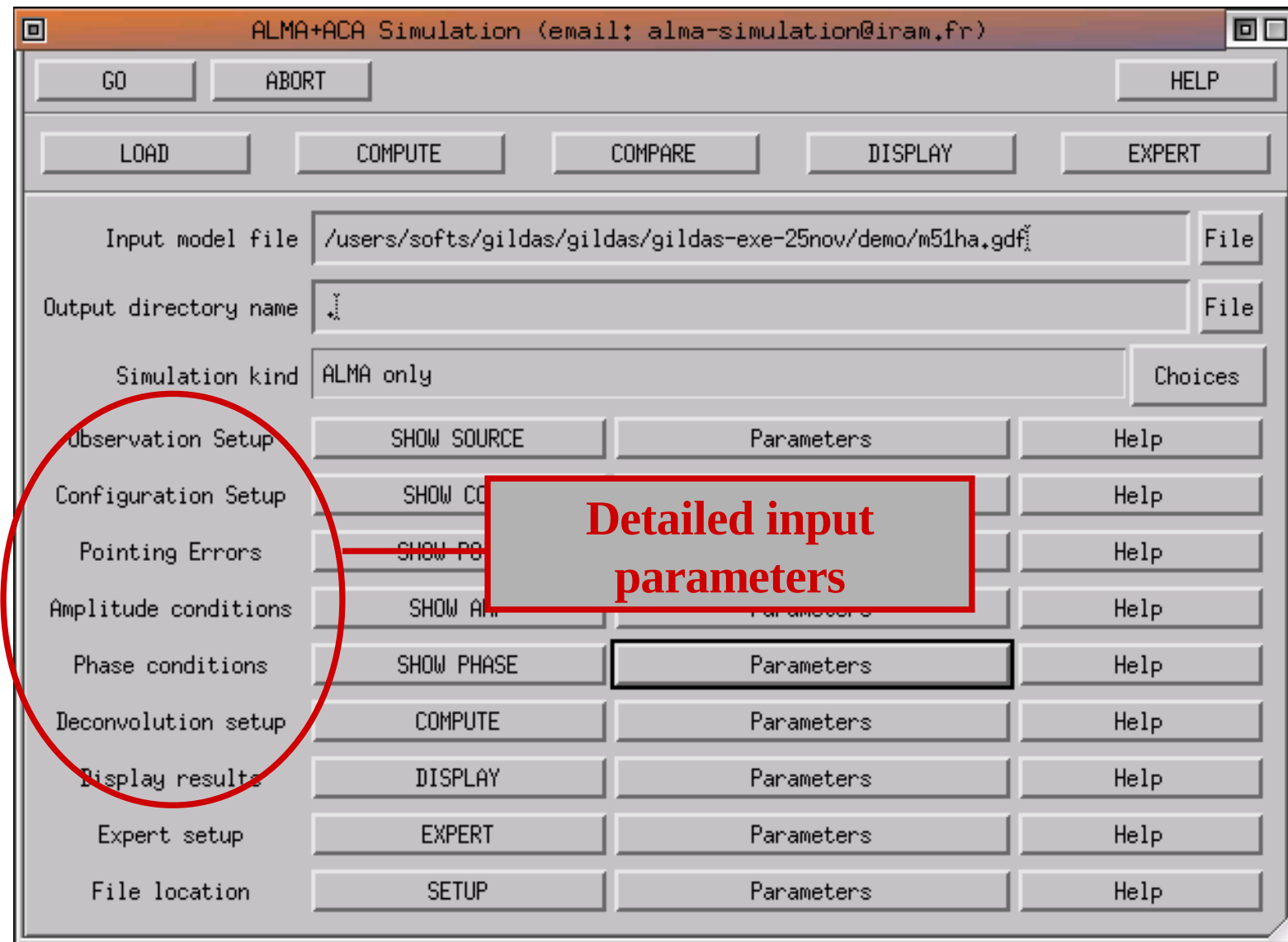
Widget Interface: I. General view



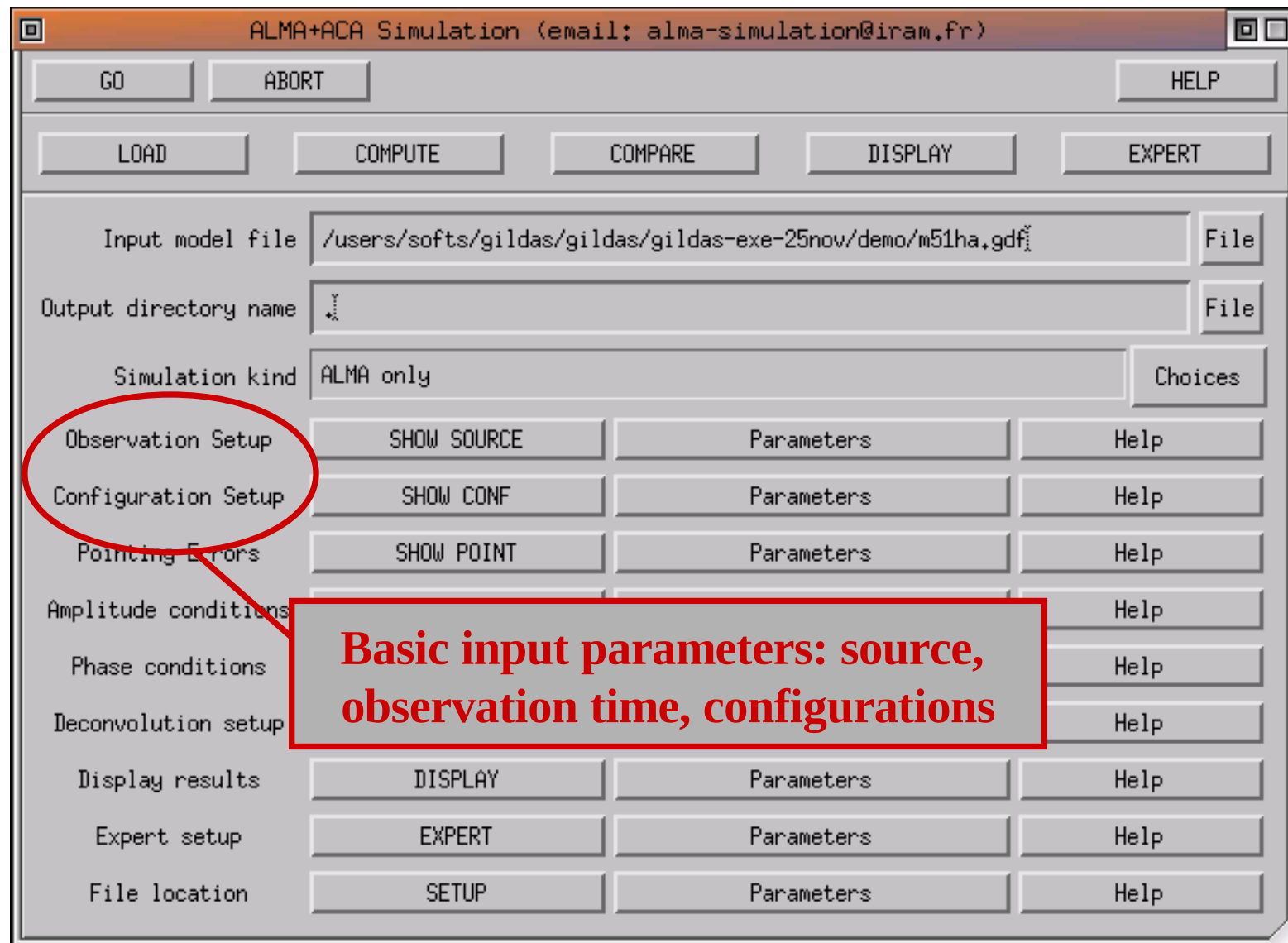
Widget Interface: II. Global parameters



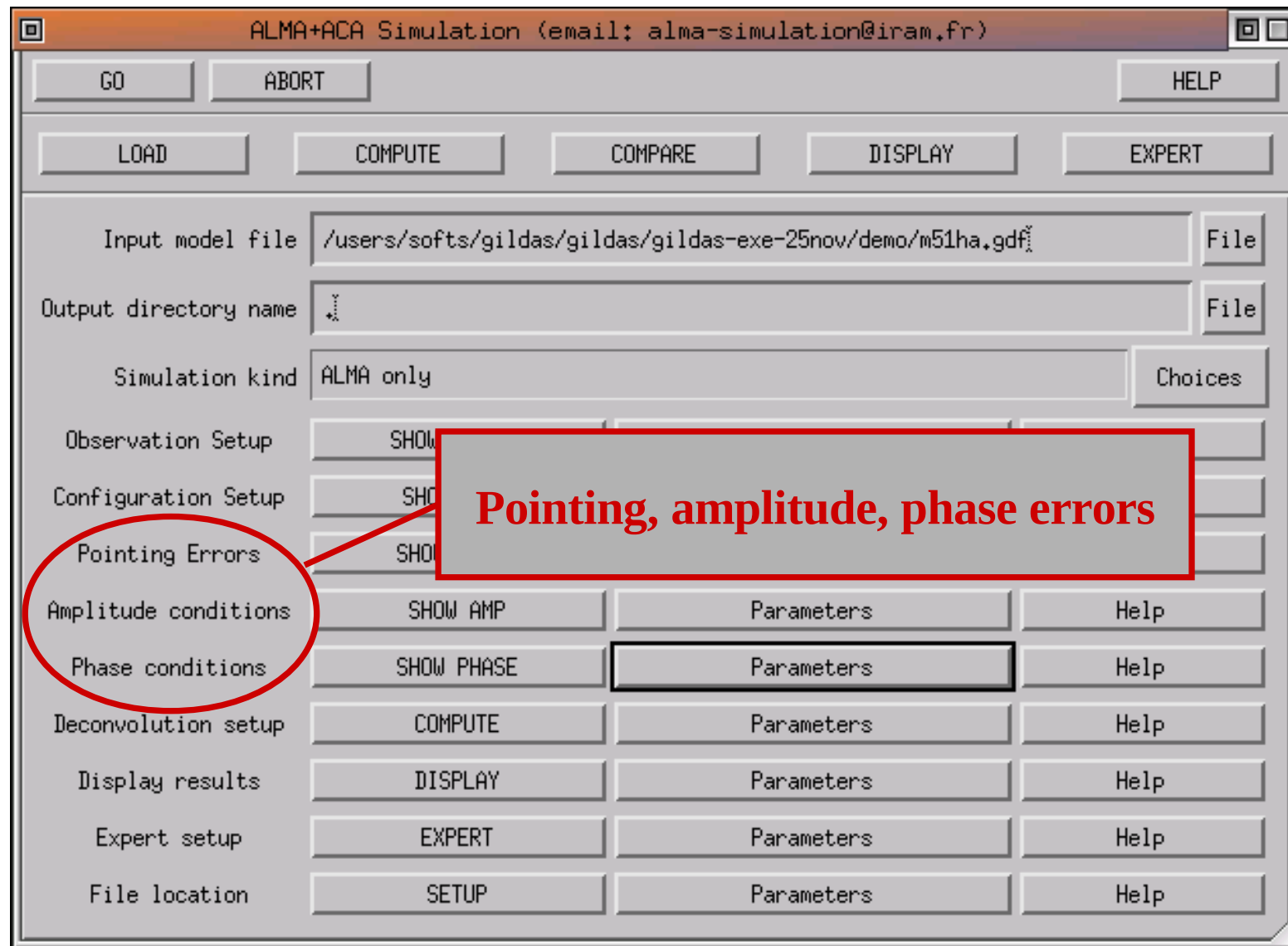
Widget Interface: III. Detailed parameters



Widget Interface: IV. Basic inputs

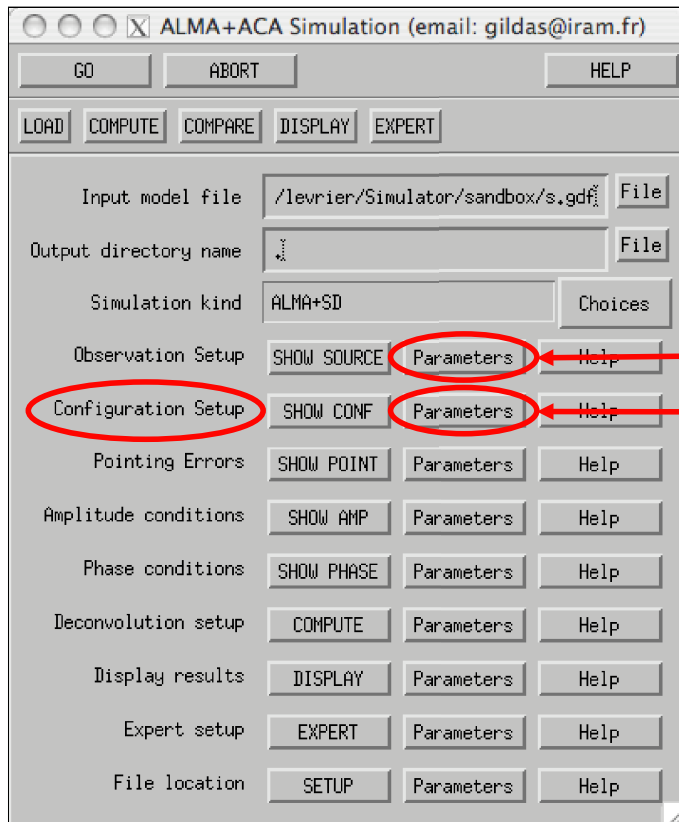


Widget Interface: V. Errors

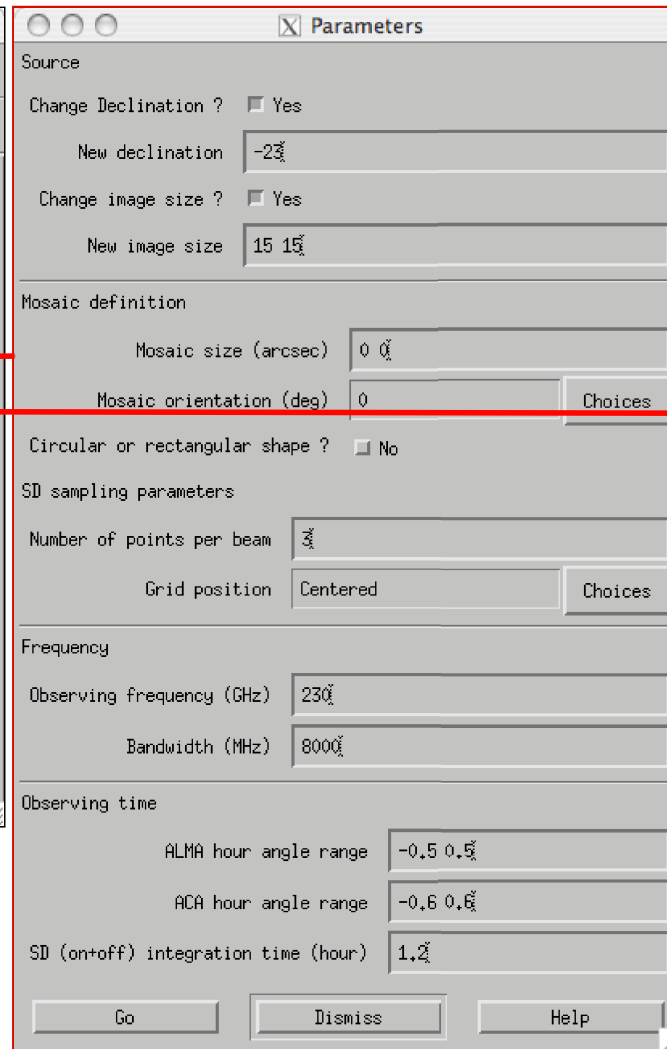


Widget Interface: VI. Additional panels

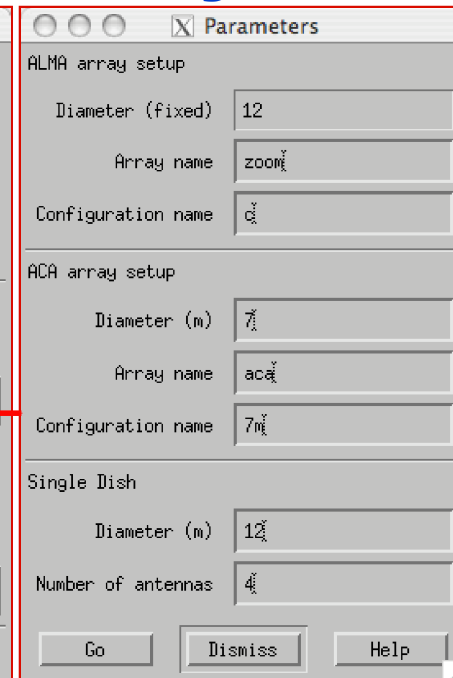
Main window



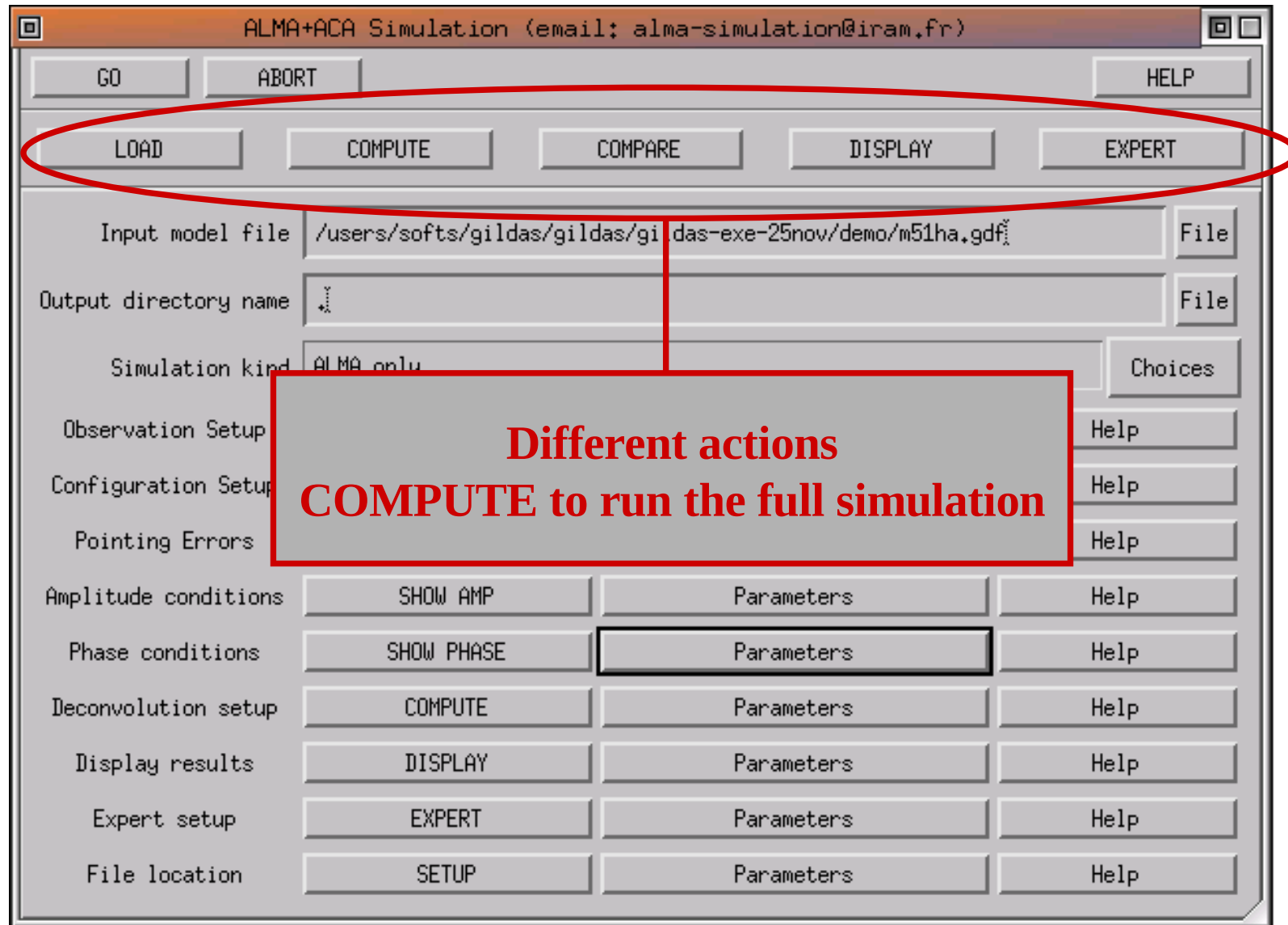
Observation



Configuration



Widget Interface: VII. Actions



Conclusion

Limitations

- No multi-configurations.
- No spectral lines.
- No polarization.

Advantages

- Integrated tool from input image to fidelity plot.
- Many possibilities.

⇒ A nice tool to prepare ALMA science.

Future Interferometric On-The-Fly (Pety & Rodriguez-Fernandez 2010)